45. Sugauchi F, Kumada H, Sakugawa H, et al. Two subtypes of genotype B (Ba and Bj) of hepatitis B virus in Japan. Clin Infect Dis. 2004;38(9):1222–8.
46. Sugauchi F, Orito E, Ichida T, et al. Epidemiologic and virologic characteristics of hepatitis B virus genotype B having the recombination with genotype C. Gastroenterology. 2003; 124(4):925–32.
47. Orito E, Mizokami M, Sakugawa H, et al. A case–control study for clinical and molecular biological differences between hepatitis B viruses of genotypes B and C. Japan HBV Genotype Research Group. Hepatology. 2001;33(1):218–23.
48. Raimondo G, Brunetto MR, Pontisso P, et al. Longitudinal evaluation reveals a complex spectrum of virological profiles in hepatitis B virus/hepatitis C virus-coinfected patients. Hepatology. 2006;43(1):100–7.
49. Chuang WL, Dai CY, Chang WY, et al. Viral interaction and responses in chronic hepatitis C and B coinfected patients with interferon-alpha plus ribavirin combination therapy. Antivir Ther. 2005;10(1):125–33.
50. Tsai SL, Liaw YF, Yeh CT, Chu CM, Kuo GC. Cellular immune responses in patients with dual infection of hepatitis B and C viruses: dominant role of hepatitis C virus. Hepatology. 1995;21(4):908–12.
51. Akuta N, Suzuki F, Hirakawa M, et al. Amino acid substitution in hepatitis C virus core region and genetic variation near the interleukin 28B gene predict viral response to telaprevir with peginterferon and ribavirin. Hepatology. 2010;52(2):421–9.
52. Fukuma T, Enomoto N, Marumo F, Sato C. Mutations in the interferon-sensitivity determining region of hepatitis C virus and transcriptional activity of the nonstructural region 5A protein. Hepatology. 1998;28(4):1147–53.
53. Akuta N, Kumada H. Influence of hepatitis B virus genotypes on the response to antiviral therapies. J Antimicrob Chemother. 2005;55(2):139–42.
54. Yu ML, Lee CM, Chuang WL, et al. HBsAg profiles in patients receiving peginterferon alfa-2a plus ribavirin for the treatment of dual chronic infection with hepatitis B and C viruses. J Infect Dis. 2010;202(1):86–92.
55. Yu JW, Sun LJ, Zhao YH, Kang P, Gao J, Li SC. Analysis of the efficacy of treatment with peginterferon alpha-2a and ribavirin in patients coinfected with hepatitis B virus and hepatitis C virus. Liver Int. 2009;29(10):1485–93.
56. Liu CJ, Chuang WL, Lee CM, et al. Peginterferon alfa-2a plus ribavirin for the treatment of dual chronic infection with hepatitis B and C viruses. Gastroenterology. 2009;136((2)):496.e3–504.e3.

The AAA-ATPase VPS4 Regulates Extracellular Secretion and Lysosomal Targeting of α-Synuclein

Takafumi Hasegawa[1]*, Masatoshi Konno[1], Toru Baba[1], Naoto Sugeno[1], Akio Kikuchi[1], Michiko Kobayashi[1], Emiko Miura[1], Nobuyuki Tanaka[2], Keiichi Tamai[2], Katsutoshi Furukawa[3], Hiroyuki Arai[3], Fumiaki Mori[4], Koichi Wakabayashi[4], Masashi Aoki[1], Yasuto Itoyama[1,5], Atsushi Takeda[1]

1 Division of Neurology, Department of Neuroscience & Sensory Organs, Tohoku University Graduate School of Medicine, Sendai, Miyagi, Japan, 2 Division of Cancer Biology and Therapeutics, Miyagi Cancer Center Research Institute, Natori, Miyagi, Japan, 3 Department of Geriatrics and Gerontology, Institute of Development, Aging and Cancer, Tohoku University, Sendai, Miyagi, Japan, 4 Department of Neuropathology, Institute of Brain Science, Hirosaki University School of Medicine, Hirosaki, Aomori, Japan, 5 National Center Hospital for Mental, Nervous, and Muscular Disorders, National Center of Neurology and Psychiatry, Kodaira, Tokyo, Japan

Abstract

Many neurodegenerative diseases share a common pathological feature: the deposition of amyloid-like fibrils composed of misfolded proteins. Emerging evidence suggests that these proteins may spread from cell-to-cell and encourage the propagation of neurodegeneration in a prion-like manner. Here, we demonstrated that α-synuclein (αSYN), a principal culprit for Lewy pathology in Parkinson's disease (PD), was present in endosomal compartments and detectably secreted into the extracellular milieu. Unlike prion protein, extracellular αSYN was mainly recovered in the supernatant fraction rather than in exosome-containing pellets from the neuronal culture medium and cerebrospinal fluid. Surprisingly, impaired biogenesis of multivesicular body (MVB), an organelle from which exosomes are derived, by dominant-negative mutant vacuolar protein sorting 4 (VPS4) not only interfered with lysosomal targeting of αSYN but facilitated αSYN secretion. The hypersecretion of αSYN in VPS4-defective cells was efficiently restored by the functional disruption of recycling endosome regulator Rab11a. Furthermore, both brainstem and cortical Lewy bodies in PD were found to be immunoreactive for VPS4. Thus, VPS4, a master regulator of MVB sorting, may serve as a determinant of lysosomal targeting or extracellular secretion of αSYN and thereby contribute to the intercellular propagation of Lewy pathology in PD.

Introduction

Although the pathophysiology of Parkinson's disease (PD) is still a topic of debate, the current consensus is that the cytoplasmic accumulation of fibrillar α-synuclein (αSYN) in the affected brain lesions is a hallmark of the initiation and progression of the disease [1,2,3,4,5]. In human brain, αSYN is enriched in presynaptic nerve terminals and is mainly detected both in cytosolic and synaptosomal fractions [6,7]. On the other hand, both monomeric and oligomeric αSYN has been found in the neuronal culture medium as well as in body fluids such as plasma and cerebrospinal fluid (CSF) [8,9,10,11]. The existence of extracellular αSYN is also supported by the fact that the hydrophobic core region of αSYN, termed NAC (non-amyloid-β component), is observed in the extracellular senile plaques of Alzheimer's disease (AD) [12]. The biochemical influence of extracellular αSYN is not understood yet, but in vitro generated soluble αSYN oligomers can induce transmembrane seeding of αSYN aggregation and eventually cause neuronal cell death [13]. The intercellular transmission of αSYN is also verified by co-culture experiments and in vivo animal models showing that αSYN aggregates released from neuronal cells can be transferred to neighboring cells and form intracellular

inclusions [14,15,16,17]. Moreover, it has been shown that αSYN-containing conditioned medium not only induced neuronal death, but also triggered inflammatory responses in astroglial cells [15]. Finally, the in vivo cell-to-cell propagation of pathogenic protein was strongly supported by recent observations showing that αSYN-positive, Lewy body-like cytoplasmic inclusions were found in fetal mesencephalic neurons that were transplanted into the brain of PD patients more than a decade ago [18,19,20]. This scenario is immensely attractive as an acceptable explanation for the clinically observed progression of neurodegenerative diseases as well as the stereotypic spread of Lewy pathology suggested by Braak and his colleagues [21].

The cellular and molecular mechanisms by which intercellular transmission of infectious prions occurs are still enigmatic. Nevertheless, several reports revealed that both normal cellular prion protein (PrPc) and the abnormally folded pathogenic form (PrPsc) were associated with nanovesicles called 'exosomes' released from non-neuronal and neuronal cells [22,23,24,25]. Once released from a cell it is proposed that exosomes could fuse with the plasma membrane of neighboring cells, transferring exosomal molecules from one cell to another. Vesicles with the hallmarks of exosomes have been detected in a large variety of

biological fluids including saliva, serum/blood, urine and CSF [26]. Very recently, it was shown that part of the cell-produced αSYN can be secreted via an exosomal, calcium-dependent mechanism and that the exosome-containing conditioned medium from αSYN-expressing cells caused the cell death of recipient neuronal cells [27]. Another piece of evidence showed that lysosomal dysfunction led to an increase in the release of αSYN in exosomes and a concomitant increase in αSYN transmission to recipient cells [28]. These findings raise the possibility that methods to prevent pathogenic protein trafficking and propagation could be designed from insights concerning the mechanisms involved in exosome biogenesis.

Multivesicular bodies (MVBs), the endocytic organelles from which exosomes are derived, are generated from the invagination of the limiting membrane into the luminal space [29,30,31]. MVBs are involved in the sequestration of proteins that are condemned to lysosomal degradation. An alternative destination of MVBs is their exocytic fusion with the plasma membrane leading to the release of intraluminal vesicles (ILVs; i.e., exosome) into the extracellular environment. Mechanistically, the sorting of cargo proteins into ILVs from MVBs is a tightly regulated process that depends on a functional complex called ESCRT (Endosomal Sorting Complex Required for Transport) [32,33,34]. This highly conserved machinery consists of three distinct but cooperative functions: first, it recognizes ubiquitylated cargo protein; second, it promotes membrane deformation, facilitating the cargo to be sorted into endosomal invaginations; third, it catalyzes the final perimeter membrane scission of the endosomal invagination, which forms ILVs containing the sorted cargo [35]. During these processes, AAA (ATPases Associated with diverse cellular Activities)-ATPase VPS4 (Vacuolar Protein Sorting 4) is required for the final ESCRT-disassembly, which completes the membrane abscission and is thus indispensable for MVB biogenesis [36]. Functional VPS4 is composed of two parallel hexameric rings made of VPS4A and B. It is known that VPS4 paralogues are differentially expressed in different organs, e.g., the expression of VPS4A is higher than that of VPS4B in mouse brain. [37].

We now report that, in contrast to PrP, extracellular αSYN was mainly detected in the supernatant fraction rather than in exosome-containing pellets from neuronal culture medium (CM) and CSF. Furthermore, perturbation of MVB-exosome genesis by dominant negative (DN) VPS4A unexpectedly increased extracellular αSYN concomitant with decreased lysosomal targeting of αSYN. The aberrant secretion of αSYN induced by VPS4 malfunction was effectively restored by the functional disruption of recycling endosome regulator Rab11a. Our results uncover a novel functional role of the MVB sorting pathway in the extracellular secretion as well as lysosomal targeting of αSYN.

Results

α-Synuclein Is Present in Endosomal Compartments

In eukaryotic cells, endosomes comprise three different compartments: early endosomes, late endosomes, and recycling endosomes. They are not only distinguished by morphology, differential density, and internal pH, but also by the specific localization of Rab GTPases [38,39]. To determine whether αSYN is actually localized in the endosomal compartment in cultured cells, we transiently transfected Myc-αSYN-expressing HEK293T and human neuronal SH-SY5Y cells together with EGFP-tagged Rab GTPase Rab5a, Rab7, and Rab11a, which are indispensable effectors/constituents of early endosomes, late endosomes, and recycling endosomes, respectively [39]. The reason why we used HEK293T cells is that they are very easy to

transfect and the level of protein expression is very high. As shown in Fig. 1A and B, exogenously expressed αSYN in both cells was clearly detected not only throughout the cytosol but also in punctate endosomal structures, which were positive for EGFP-Rab5a, Rab7, and Rab11a. The partial co-localization of endogenous αSYN with endosomal Rab proteins was also observed in human neuronal SH-SY5Y cells (Fig. 1C). The patterns of distribution of EGFP-tagged Rab family proteins were quite distinct from those of the EGFP-expressing cells, showing diffuse cytoplasmic signals throughout the cytosol (data not shown).

α-Synuclein Is Detected in Supernatant But Not in Exosome-Containing Pellet from Neuronal Culture Medium and CSF

To investigate whether αSYN is released in association with exosomes into the extracellular milieu, we induced wt and A53T mutant αSYN expression in SH-SY5Y cells and examined the CM as well as whole cell lysates for the presence of αSYN (Fig. 2A). The collected medium was further separated into the supernatant and an exosome-containing pellet, and the successful separation was verified using the exosome marker Alix. After induction, αSYN monomer and high molecular weight (HMW) αSYN smear were significantly increased in the cell lysates. A53T mutant αSYN had a high propensity to form HMW smear, as previously reported [2,40]. Following the induction, wt and, to a lesser extent A53T mutant αSYN, in the supernatant of CM were easily detected and dramatically increased. However, the expression levels of αSYN in the exosome-containing pellet were very weak and unchanged even after the induction. Thus, it is supposed that the majority of secreted αSYN in CM is not concealed in exosome vesicles, but released directly into the supernatant. We confirmed that the presence of αSYN in CM was not attributable to disruption of the cellular membrane since Hsp90, the most abundantly expressed protein in the cytosol of eukaryotic cells, could not be detected in the samples prepared from CM. To confirm the extracellularαSYN localization in more detail, the resuspended exosome-containing $100,000 \times g$ pellets obtained from CM were further analyzed by floatation in a continuous sucrose-density gradient (Fig. 2B). As expected, Western blot analysis of the separated fractions revealed that PrP migrated near the top of the density gradient with concomitant enrichment of the exosome-associated proteins, Alix and Flottilin-1. By contrast, only trace amounts of αSYN were broadly detected in the sucrose gradient and no exosomal enrichment was observed. The separation appeared to be successful since exosomes have been reported to float on sucrose gradients at density ranges depending on the cell type [41].

PrP can be detected in several biological fluids such as blood, lymph, and CSF, which are confirmed to be sources of prion infectivity [42]. Furthermore, exosomes isolated from ovine CSF were an efficient means of enriching PrPc and PrPsc suitable for detection using Western blot analysis [41]. While detectable amounts of αSYN have also been identified in human blood plasma and CSF [8,9,10,11], it has not yet been determined whether αSYN is enriched in exosomes derived from CSF. In an attempt to examine whether CSF-derived exosomes were enriched in αSYN relative to neat CSF, we pooled CSF samples from five different PD patients together with age-matched controls and then the exosomes were isolated by ultracentrifugation. Equal concentrations (50 µg per lane) of total CSF samples were loaded alongside CSF-derived exosomes and then probed with anti-αSYN and PrP antibodies (Fig. 2C). The amount of PrP detected in CSF-derived exosomes was enriched compared to neat CSF in which
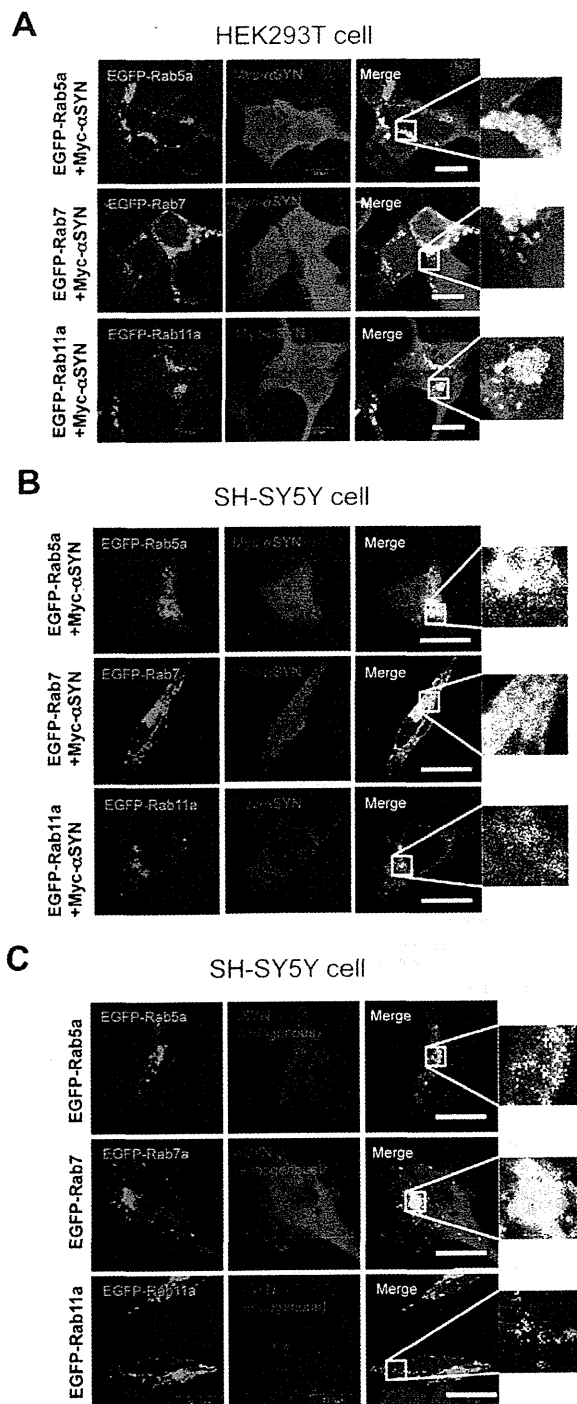
A

HEK293T cell

B

SH-SY5Y cell

C

SH-SY5Y cell

Figure 1. α-synuclein is present in endosomal compartments. Colocalization experiments of Myc-tagged αSYN (red) with endosome-associated EGFP-tagged Rab proteins (green) in HEK293T cell (*A*) and SH-SY5Y dopaminergic neuronal cells (*B*). The subcellular distribution of endogenous αSYN was also examined in SH-SY5Y cells expressing EGFP-tagged Rab proteins (*C*). Cells were fixed 48 hours post-transfection and were subjected to immunofluorescent analysis. In both cell lines, exogenously expressed αSYN was detected not only throughout the cytosol but also in punctate endosomal structures that were positive for

EGFP-Rab5a (early endosome marker), Rab7 (late endosome marker), and Rab11a (recycling endosome marker), respectively. Nuclei were conterstained with TO-PRO3 iodide (pseudocolored blue). The inset picture is a magnified picture of the square area. Immunostaining was performed three times and the experiment three times with the same results. Size bar: 10 μm.

signals were only weakly observed. We confirmed that αSYN was weakly but specifically detected in neat CSF; however, we failed to detect αSYN-positive signals in CSF-derived exosomes by standard immunoblotting technique. There was no significant difference in the expression levels of CSF αSYN between PD patients and normal controls.

Expression of DN VPS4A Leads to Increased Extracellular α-Synuclein and a Parallel Decrease in Lysosomes

Exosomes, by definition, correspond to the ILV of MVB, and therefore targeting a component of the ESCRT machinery could be used to interrupt protein sorting to ILV and exosome formation [22,30]. In fact, it has been shown that disturbed ILV formation by the over-expression of DN-VPS4A induced PrPc entrapment at the limiting membrane of endosomes in rabbit epithelial Rov9 cells [43]. Thus, we hypothesized that, if αSYN secretion largely depends on exosomes as well as PrPc, functional disruption of the ESCRT components by DN-VPS4A could decrease extracellular αSYN. To prove this, αSYN-expressing HEK293T cells were co-transfected either with 3XFLAG-tagged wt-VPS4A or DN mutant (E228Q) VPS4A harbouring a single amino acid exchange in its AAA domain [44]. Forty-eight hours post-transfection, the cells were harvested and sequentially fractionated into cytosolic, endosomal, and lysosomal fractions. In parallel, proteins in cultured medium were isolated by TCA/acetone precipitation. All samples were subjected to immunoblot analysis and the relative purity of the fractions was assessed using antibodies against specific markers including LAMP-1 (lysosome), Rab5 (early endosome), Rab11 (recycling endosome), Hsp90 (cytosol), and BSA (CM), respectively. The results, shown in Fig. 3A, revealed that exogenous expression of DN-VPS4A, and a lesser extent wt-VPS4A, caused an unexpected increase of both monomeric and oligomeric αSYN in CM compared to mock (3XFLAG peptide)-transfected control. The partial increase of αSYN secretion by wt-VPS4A expression could be explained by previous data demonstrating that even wt-VPS4A was able to negatively perturb the ESCRT pathway when heavily over-expressed [45]. An intriguing finding was that the increased αSYN secretion into CM was accompanied by a slight decrease of lysosomal HMW αSYN smear (i.e., oligomers), since the autophagic-lysosomal pathway had been thought to be essential for the clearance of αSYN aggregates [46,47,48]. In accord with these findings, we confirmed that bafilomycin A1, a cell-permeant inhibitor of vacuolar type H+-ATPase, which plays a pivotal role in acidification and protein degradation in lysosomes, induced the buildup of cellular αSYN oligomers in parallel with the increase of its extracellular secretion in a dose-dependent manner (Fig. 3B). It is also interesting to note that the accumulated αSYN oligomers in HEK293T cells were prominent in CM, endosomal, and lysosomal compartments compared to those in the cytosol, which is in good agreement with a previous study showing that αSYN is more prone to aggregate in vesicular structures compared to the cysotol [49]. Also note that endosomal proteins including αSYN seemed to be heavily ubiquitylated compared to αSYN in other fractions. As previously reported, immunostaining revealed that exogenous expression of DN-VPS4A in HEK293T cells led to the appearance
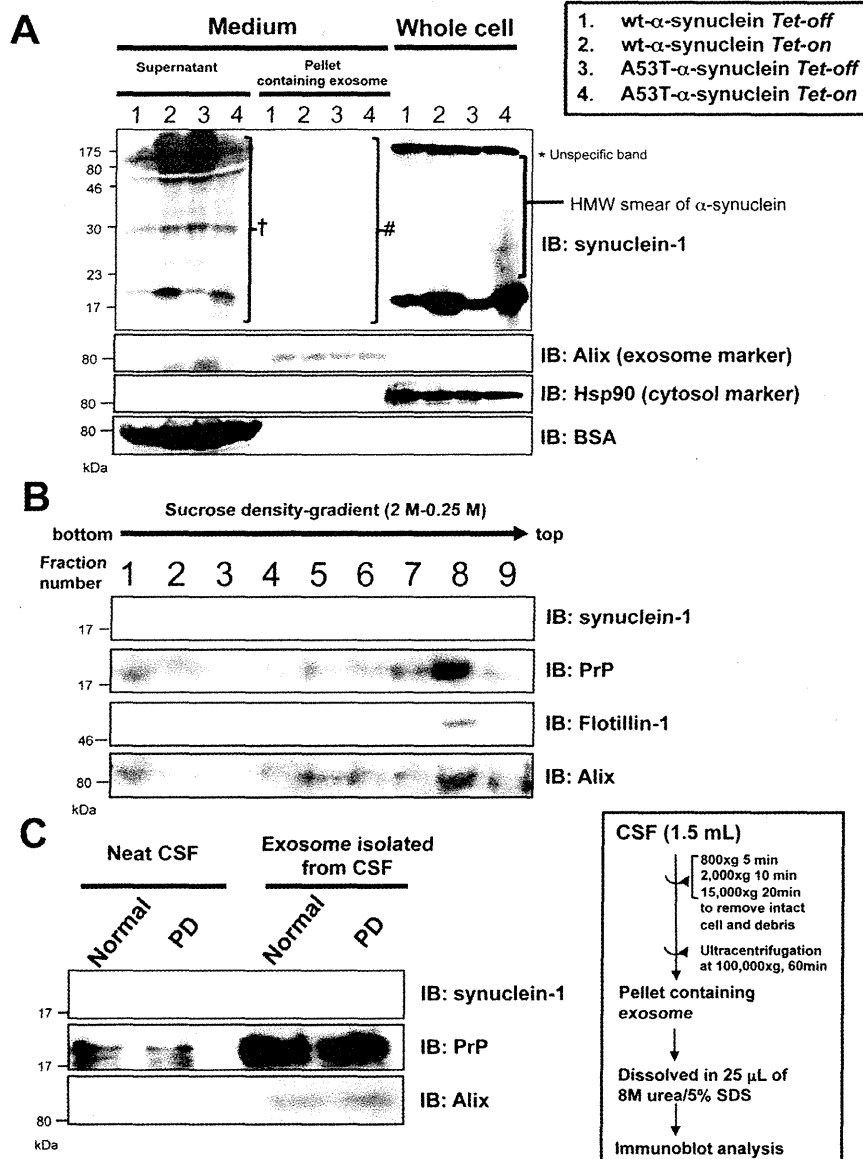
Figure 2. α-synuclein is detected in supernatant but not in the exosome-containing pellets from neuronal culture medium and CSF by standard immunoblot analysis. A. wt and A53T mutant αSYN were inducibly expressed in SH-SY5Y cells for 48 hours. Culture medium as well as whole cell lysates (50 μg protein per lane) were subjected to Western blot analysis. The collected media were further separated into the supernatant and exosome-containing pellets before loading onto gels. Alix, Hsp90, and BSA were used as markers for exosome, cytosol, and culture medium, respectively. In the neuronal culture medium, both monomeric/oligomeric wt and mutant αSYN were recovered in the supernatant (dagger) rather than exosome-containing pellets (hash). Asterisk indicates unspecific band. B. The resuspended exosome-containing pellets from the culture medium were further separated by sucrose-density gradient followed by Western blot analysis. Immunoblot probed with synuclein-1 anti-αSYN, anti-PrP Abs and the successful separation of exosome was confirmed by exosomal markers, Flotillin-1 and Alix. As shown in the blot, PrP migrated near the top of the density gradient (fraction #8) with concomitant enrichment of exosome-associated proteins. By contrast, no exosomal enrichment was observed with αSYN. C. CSF (1.5 mL) from 5 PD patients together with age-matched controls was pooled and exosome-containing pellets were isolated by successive centrifugation indicated. Equal concentrations (50 μg per lane) of total CSF samples were loaded alongside CSF-derived exosomes and then probed with anti-αSYN and PrP antibodies. PrP detected in CSF-derived exosomes was enriched compared to neat CSF. αSYN was weakly but specifically detected in neat CSF, whereas no αSYN-positive signal could be detected in CSF-derived exosomes. No significant difference was observed in the expression levels of CSF αSYN between PD patients and normal controls. Representative Western blots from three independent experiments are presented.
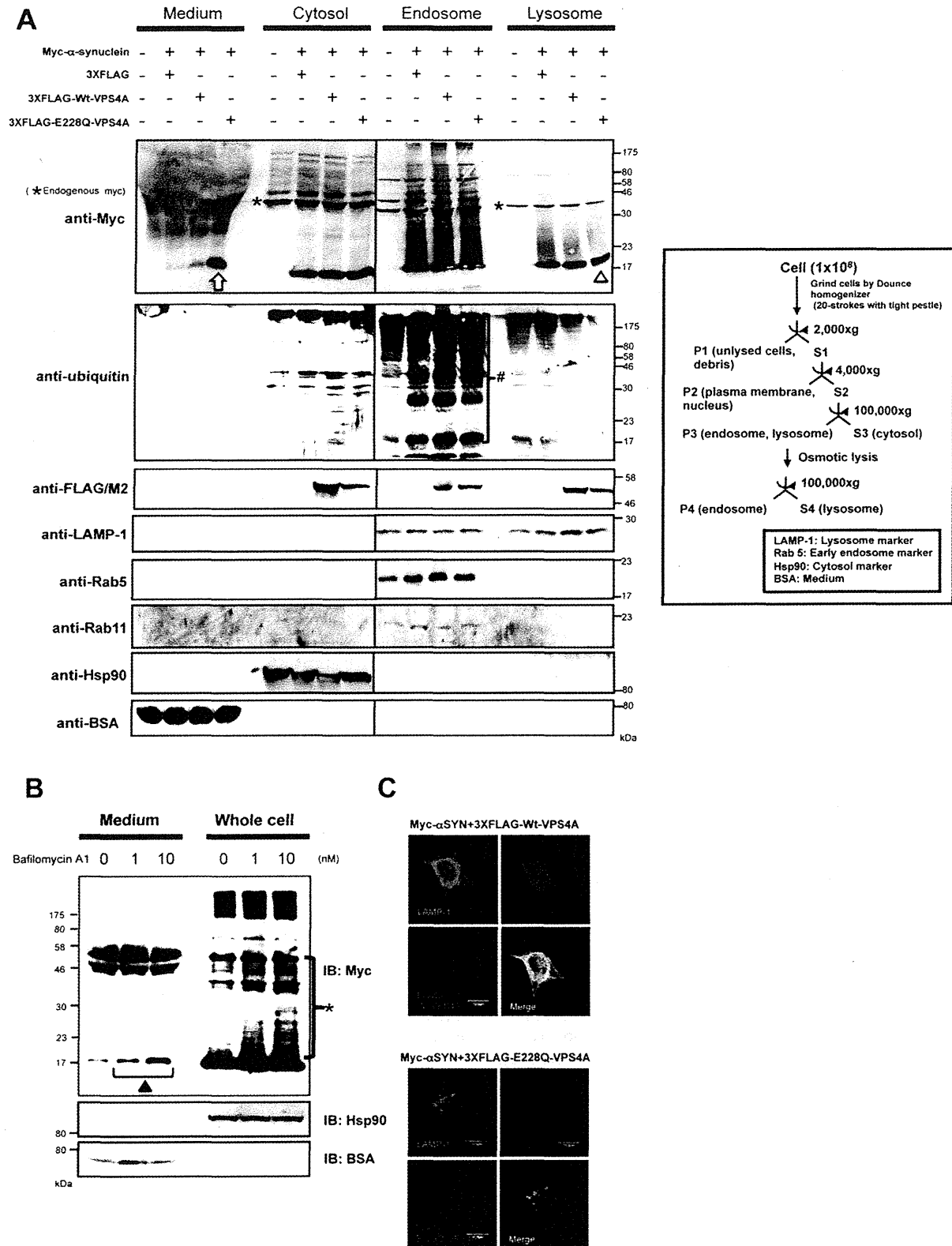doi:10.1371/journal.pone.0029460.g002

Figure 3. Over-expression of DN VPS4 in HEK293T cells leads to increased extracellular α-synuclein and parallel decrease in lysosome. *A.* αSYN-expressing HEK293T cells were co-transfected either with 3XFLAG-tagged wt-VPS4A or DN mutant (E228Q) VPS4A. Forty-eight hours after transfection, HEK293T cells were fractionated into the cytosol (S3), endosome (P4), and lysosome (S4). Fractionated cell lysates as well as protein extracts from the culture medium (50 μg protein per lane) were subjected to Western immunoblot analysis using anti-Myc, anti-ubiquitin, anti-FLAG/M2 Abs. Each fraction was verified by the presence of a specific marker protein: LAMP-1 (late endosome and lysosome), Rab5 (early endosome), Rab11 (recycling endosome), Hsp90 (cytosol), and BSA (culture medium). As shown in the blot, marked increase of extracellular αSYN monomer and multimers (*white arrow*) concomitant with slightly decreased lysosomal αSYN-immunopositive smear (*open triangle*) were observed by over-expression of DN VPS4A. Note that endosomal proteins including αSYN seemed to be heavily ubiquitylated (*hash*). Asterisk indicates endogenous myc band. *B.* Treatment with lysosomal inhibitor bafilomycin A1 (0–10 nM) for 24 hours induced the buildup of cellular αSYN oligomers (*asterisk*) in parallel with the increase of extracellular αSYN monomer (*closed triangle*). *C.* Subcellular localization of Myc-αSYN (red) in HEK293T cells expressing wt or DN VPS4A (*magenta*). LAMP-1 (*green*) was used as a marker for late endosome and lysosome. DN VPS4 distibuted as aberrant cytoplasmic punctate structures, showing a marked contrast to wt-VPS4A with diffuse perinuclear distribution. Representative Western blots from three separate experiments are shown. Scale bar: 10 μm.
doi:10.1371/journal.pone.0029460.g003

of aberrant cytoplasmic punctate structures, providing a distinct contrast to the diffuse perinuclear distribution of wt-VPS4A (Fig. 3C) [43]. We confirmed that the aberrant secretion of αSYN by DN-VPS4A expression was not a cell-type-specific phenomenon in HEK293T cells since we observed an identical result in SH-SY5Y neuronal cells, namely, wt as well as A53T mutant αSYN secretion was significantly increased by the nucleofection of wt- and DN-VPS4A (Fig. 4A). Note that the extracellular secretion of monomeric wt-αSYN was much higher than that of A53T mutant αSYN in mock-transfected cells as well as in DN-VPS4A engineered cells (Fig. 4B). Nucleofection of SH-SY5Y cells using the Nucleofector device provided a technique for introducing constructs into SH-SY5Y cells with ~70% efficiency as estimated from the EGFP fluorescence at 48 hours post-transfection (our unpublished data).

VPS4 is found in the core structures of Lewy bodies

As shown in Fig. 3A, we found that αSYN in endosome and lysosome is more prone to aggregate than in cytosol. This result implies that endosomal/lysosomal organelles containing αSYN aggregates might be the potential source of Lewy bodies. To prove this, the substantia nigra and the temporal lobes from four patients with PD and four age-matched controls dying from known, non-neurological causes were subjected to immunohistochemical analysis using anti-human VPS4 Ab. In all brain tissues from PD patients, the core structures of Lewy bodies showed VPS4 immunoreactivity (Fig. 5), whereas only weak background staining was observed in control brain sections (data not shown). The percentage of VPS4-immunoreactive Lewy bodies in the substantia nigra (A and B) and the temporal lobes (C and D) of four PD brains are 90% and 10%, respectively.

Increased Secretion of α-Synuclein by DN-VPS4A Is Restored by DN-Rab11a

It was shown that αSYN incorporated from the extracellular space was able to be resecreted out of neurons via a process modulated by recycling endosome regulator Rab11a [50]. To test the possible implication of the Rab11a-dependent recycling pathway in the secretion of αSYN *in vivo*, αSYN-expressing HEK293T cells were co-transfected with EGFP, EGFP-tagged wt-Rab11a, Q70L constitutively active (CA)-Rab11a, or S25N DN-Rab11a construct, respectively (Fig. 6). The S25N point mutation in Rab11a has been known to increase its activity for GDP, thereby locking the Rab GTPase in an inactive, non-membrane-associated state [51]. In comparison with EGFP, wt-Rab11a, and CA-Rab11a expressing cells, the cells expressing DN-Rab11a showed a slight decrease of the extracellular oligomeric αSYN in CM as well as the appearance of αSYN-immunopositive HMW smear in the endosome and, to a lesser extent, cytosolic and

lysosomal fractions. This finding indicated that a part of endogenous αSYN was trafficked via a recycling endosome pathway for extracellular secretion, and the reduced recycling efficiency by DN-Rab11a expression would probably yield the aberrant retention of αSYN both in endosomes and lysosomes. Given the role of Rab11a in regulating the secretion of cellular αSYN, we speculated that the Rab11a-regulated recycling pathway could also be involved in the hypersecretion of αSYN from HEK293T cells transfected with DN-VPS4A. To test this, HEK293T cells doubly expressing αSYN and DN-VPS4A or SH-SY5Y neuronal cells expressing DN-VPS4A were further co-transfected with DN-Rab11a that lacks GTP-binding activity, then whole cell lysates as well as CM were subjected to immunoblot analysis (Fig. 7A and B, respectively). As shown in the blots, the augmented secretion of over-expressed and endogenous αSYN induced by VPS4 malfunction were effectively restored by the co-expression of GDP-locked DN-Rab11a, whereas the total cellular levels of αSYN remained unchanged.

Discussion

Until recently, αSYN has been considered to exert its physiological as well as pathogenic effects intracellularly. However, accumulating evidence suggests that both monomeric and oligomeric αSYN can be secreted into the extracellular environment, thereby affecting the normal physiological state of neighboring neuronal and glial cells [17]. In the case of prion protein, cell-to-cell transmission by means of exosome shuttle, caveolae-mediated endosomal pathway, and tunneling nanotubes has been suggested [23,25,52,53]. Therefore, it is tempting to speculate that similar mechanisms could be involved in the transmission of other amyloidogenic proteins. Given that the prion enrichment and infectivity were confirmed in the cell culture media of infected cells as well as body fluids from suffering animals, prion transfer could occur by a process other than through direct cell contact [25,41,43]. In addition to prion protein, several reports suggested that exosomes may serve as vehicles for the transcellular spread of amyloidogenic proteins in neurodegenerative diseases including PD [17,54,55,56]. As reported previously [23,24,25], we found a striking condensation of prion in exosomes in CM and human CSF, whereas such enrichment was not observed with αSYN (Fig. 2A, 2B and 2C). The marked discrepancy in terms of the exosomal localization implies that the secretory mechanism of αSYN might be different from that of prion protein. This idea is also supported by our findings showing that, in contrast to prion protein, the suppression of MVB-exosome biogenesis by DN VPS4A significantly increased the extracellular αSYN in non-neuronal and neuronal cells (Fig.3A and 4A). It is true that our results would seem to conflict with previous reports demonstrating that αSYN is secreted from
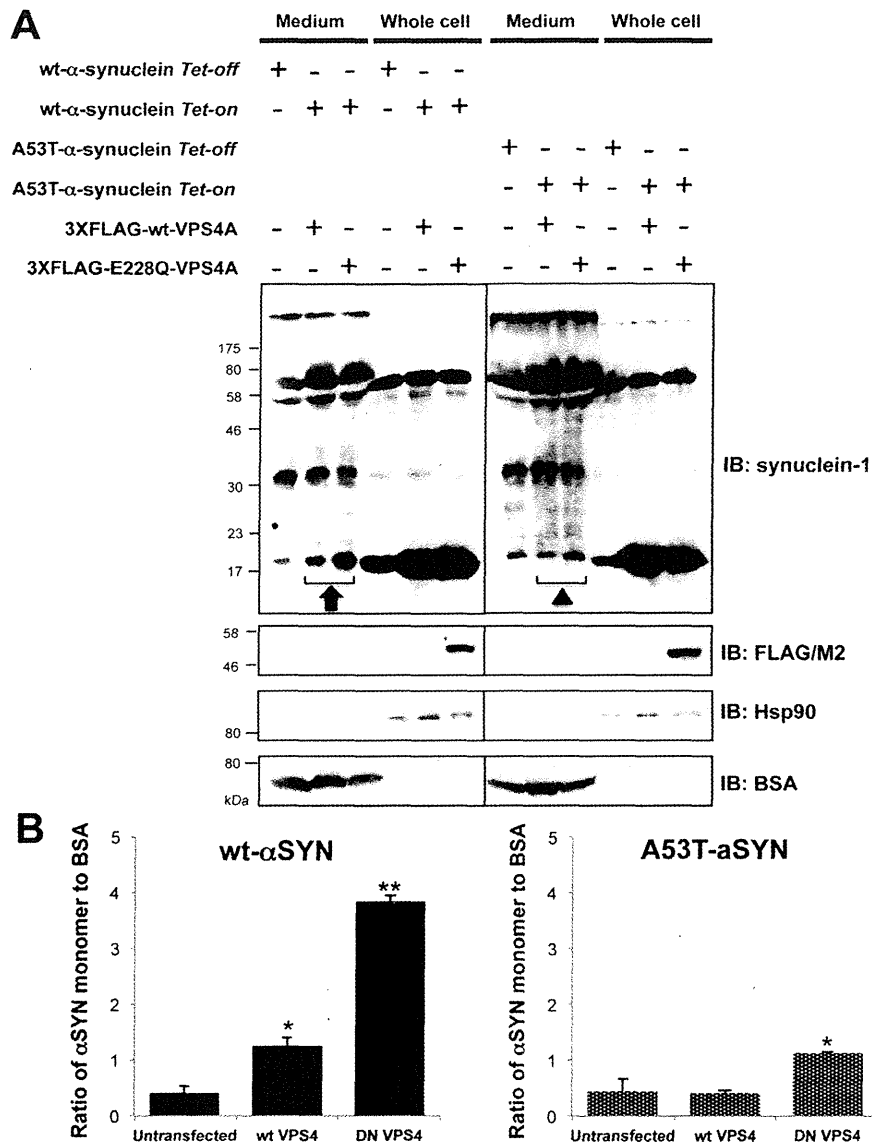
Figure 4. Expression of DN VPS4A increases wt as well as A53T mutant α-synuclein in SH-SY5Y neuronal cells. *A.* SH-SY5Y cells inducibly expressing wt or A53T mutant αSYN were further co-transfected with 3XFLAG-tagged wt or DN E228Q mutant VPS4A plasmids. After 48 hours of αSYN induction with doxycycline, whole cell and proteins from culture media (50 μg protein per lane) were subjected to immunoblot analysis using anti- synuclein-1 and anti-FLAG/M2 antibody. Hsp90 and BSA were used as markers for cytosol and culture medium, respectively. Increased extracellular secretion of wt and A53T mutant αSYN were observed by DN VPS4A. Note that the extracellular secretion of monomeric wt-αSYN (*black arrow*) was higher than that of A53T mutant αSYN (*closed triangle*) in mock-transfected cells as well as in DN-VPS4A engineered cells. Representative immunoblots from three independent experiments are shown. *B.* Densitometric measurement of monomeric αSYN secreted into culture media. Values indicate the ratio of αSYN monomer to BSA. Significant increase of wt as well as A53T αSYN in culture media was observed by co-expression of wt and or DN VPS4A (*$p<0.05$, **$p<0.005$).
doi:10.1371/journal.pone.0029460.g004

neuronal cells by exosomes under both physiological and pathological conditions [27,28]. However, it remains possible that αSYN might be secreted through different secretory pathways depending on the size of the aggregates or cellular condition. Indeed, part of the newly synthesized αSYN was rapidly secreted from MES cells via unconventional, endoplasmic reticulum/ Golgi-independent exocytosis [49]. Another study has demonstrated that the internalized extracellular αSYN was resecreted out of neurons via a process modulated by the recycling endosome

regulator Rab11a [50]. The functional importance of the recycling pathway was also verified in the cellular trafficking of amyloid-β precursor protein [57]. Our result showing that DN-Rab11a restored the aberrant αSYN secretion triggered by impaired MVB genesis also supports the functional relevance of the recycling pathway in αSYN secretion. Supposedly, under the physiological state, endosomal αSYN is destined for lysosomal degradation (Fig. 8A) or introduced into the extracellular milieu through the Rab11a-dependent recycling endosomal pathway (Fig. 8B) and, to
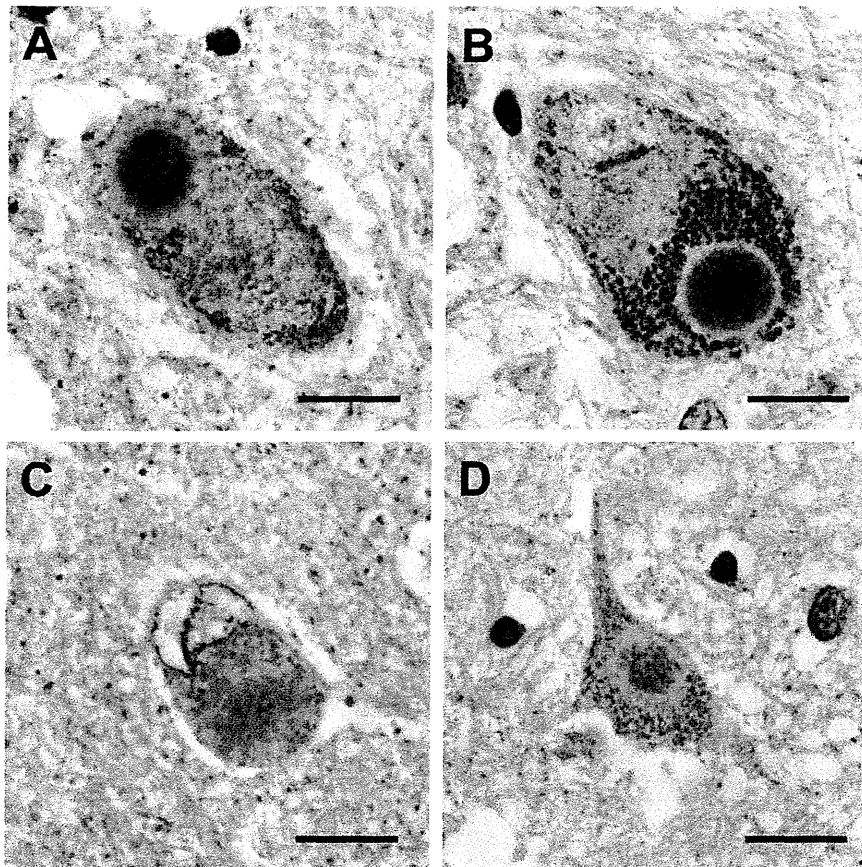
Figure 5. VPS4 was found to be a component of Lewy body. Paraffin embedded sections including the substantia nigra and the temporal lobes from four patients with PD with a mean age of 77.5 years and the controls with a mean age of 77.3 years were subjected to immunohistochemical analysis using anti-human VPS4 Ab. Diaminobenzidine were used to visualize the staining and nuclei were counterstained with hematoxylin. In all brain tissues from patients with PD, the core structures of Lewy bodies showed VPS4 immunoreactivity (Fig. 5). Only weak background staining was observed in control brain sections (data not shown). The percentage of VPS4-immunoreactive Lewy bodies in the substantia nigra (A and B) and the temporal lobes (C and D) of PD brains were 90% and 10%, respectively. Scale bar: 20 μm.
doi:10.1371/journal.pone.0029460.g005

a lesser degree, MVB-exosome pathway (Fig. 8C). However, if the intracellular αSYN reaches a toxic level or the MVB sorting pathway is dammed up for any reason, a torrent of endocytic αSYN may flow out mainly through the recycling endosome pathway. Perhaps the recycling pathway might serve as a "vent" to discharge excess αSYN that would be potentially harmful to cells. Another important finding observed in this study is that the extracellular secretion of wt-αSYN was constitutively higher than A53T mutant αSYN in mock-transfected cells as well as in DN-VPS4A engineered cells. This finding is interesting when considering the cytotoxic property of mutant αSYN, which might be liable to be entrapped inside the cells and eventually lead to cell-autonomous degeneration. It should be noted that we used cell lines over-expressing αSYN in some experiments of this study. Therefore, we cannot completely exclude the possibility that over-expressed αSYN itself might somehow affect its subcellular distribution since over-expression of αSYN hinders vesicle trafficking and recycling as a result of interaction with prenylated Rab acceptor protein 1 [58].

Since αSYN does not contain a predicted transmembrane domain or known lipid anchor, there remains a fundamental

question on how it associates with endosomal vesicles. It is known that the amino-terminal amphipathic α-helical domain of αSYN is quite similar to the class A2 α-helix found in the lipid-binding motif of several apolipoproteins [59]. In fact, αSYN binds artificial liposomes containing phospholipid vesicles with acidic head groups, lipid droplets, and lipid rafts [49]. It has been shown that the portion of αSYN stably cofractionated with vesicles from brain tissues and cultured neuronal cells was not only bound to the outer membrane but certainly localized in the vesicle lumen [49]. Therefore, αSYN might be integrated into vesicles in at least two different ways. Namely, some are loosely bound to the surface of vesicles where the interaction is controlled in the balance of the free cytosolic αSYN. The others are incorporated and sequestrated into the lumen of vesicles. The mechanism by which cytosolic αSYN moves into the endosomal vesicle is poorly understood; however, apart from the vesicle permeabilization by protofibrillar αSYN [60,61], intracellular αSYN exocytosed into the extracellular space could be internalized and directly packaged into the endosomal vesicles [15,49,62]. Intriguingly, it is known that the aggregation of αSYN was faster and more robust in the vesicles than in the cytosol [49,63]. We also observed a noticeable
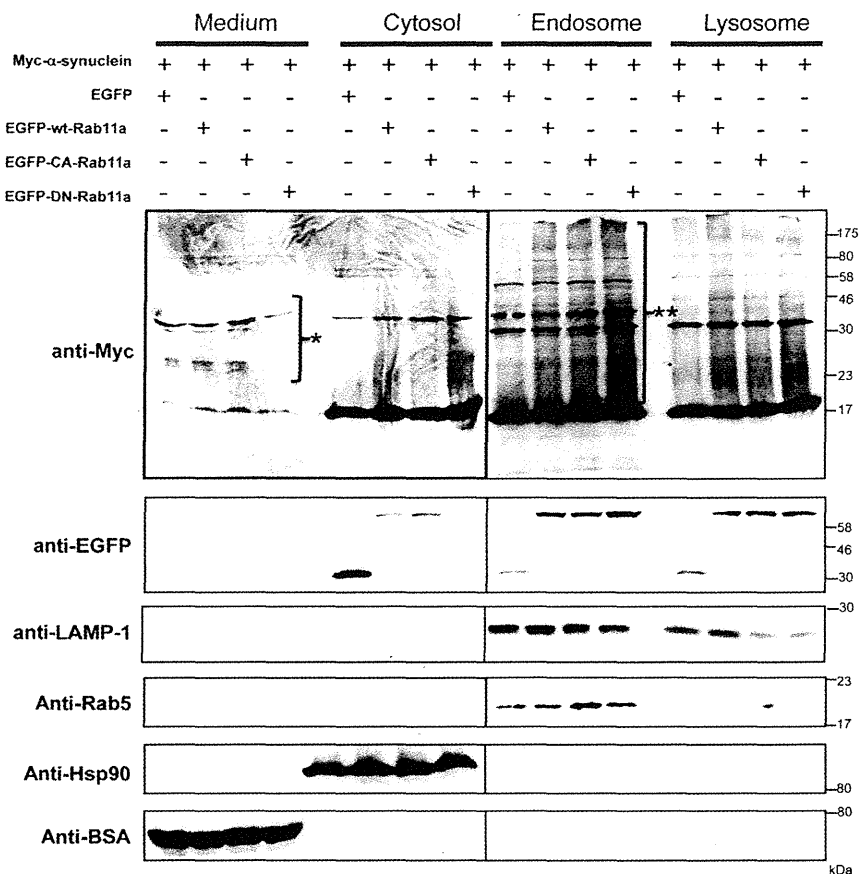
Figure 6. Part of the cellular α-synuclein was trafficked via a recycling endosome pathway for extracellular secretion. HEK293T cells expressing Myc-αSYN were co-transfected with mock (EGFP), EGFP-wt-Rab11a, EGFP-CA-Rab11a, or EGFP-DN-Rab11a expression plasmids. At 48 hours following transfection, the cells were harvested and fractionated into cytosol, endosome, and lysosome. Fractionated samples as well as total proteins from the culture media (50 μg per lane) were subjected to immunoblot analysis using anti-Myc, anti-EGFP Abs. A successful fraction was verified by the presence of a specific marker proteins. As shown in the blot, secretion of αSYN oligomer in culture medium was partly reduced by the over-expression of GDP-locked DN-Rab11a (asterisk), accompanied by the extensive retention of HMW αSYN species in the endosome (double asterisk). Representative blots from three separate experiments are shown.
doi:10.1371/journal.pone.0029460.g006

aggregation tendency in endosomal/lysosomal αSYN and the core structures of Lewy bodies showed immnoreactivity with VPS4 Ab. These findings are interesting when considering the biogenesis of Lewy bodies, because the pale body, an early cytoplasmic change before Lewy body maturation, often contains ubiquitinated proteins as well as lysosomes and vacuolar structures [64,65]. It is uncertain why intravesicular αSYN has a high propensity to form aggregates. However, specific environments inside the vesicle such as a high calcium concentration and low pH as well as the molecularly crowded milieu might synergistically promote αSYN fibrillization [66,67,68,69]. In addition, the extensive ubiquitination of endosomal αSYN found in this study may indicate a role for ubiquitin in αSYN sorting along the endosomal pathway, since multiple monoubiquitylation and Lys-63-linked polyubiquitylation have been recognized as important sorting signals for cargo proteins in the endosome membrane [33,70].

In summary, we found that impaired MVB-exosome biogenesis by DN VPS4A strikingly increased extracellular αSYN, which was correlated with the decreased lysosome-resident αSYN. The inhibited recycling efficiency by DN-Rab11a can not only cause

a decrease of the extracellular αSYN oligomer but also restore the hypersecretion of αSYN by DN-VPS4A. Furthermore, VPS4 was found to be a component of the nigral as well as the cortical Lewy bodies. Our results demonstrate how failure of the MVB sorting machinery contributes to the extracellular secretion as well as lysosomal targeting of αSYN and may thus be involved in the propagation of Lewy pathology in PD. The importance of the endosomal/lysosomal transport system in the pathogenesis of PD is also highlighted by very recent findings that a mutation in VPS35 gene encoding a retromer complex involved in the retrograde transport of proteins from the endosome to the trans-Golgi network causes late-onset familial PD [71,72]. Furthermore, in a manner similar to vaccination therapy, a reduction of the extracellular αSYN brain burden by regulating the MVB sorting could be a novel therapeutic strategy for PD and other synucleinopathies. Although the concept of prion-like propagation has been recognized as a common phenomenon in many neurodegenerative diseases, it is likely that the molecular mechanisms underlying the spreading of protein-misfolding may differ depending on the biochemical nature of the protein
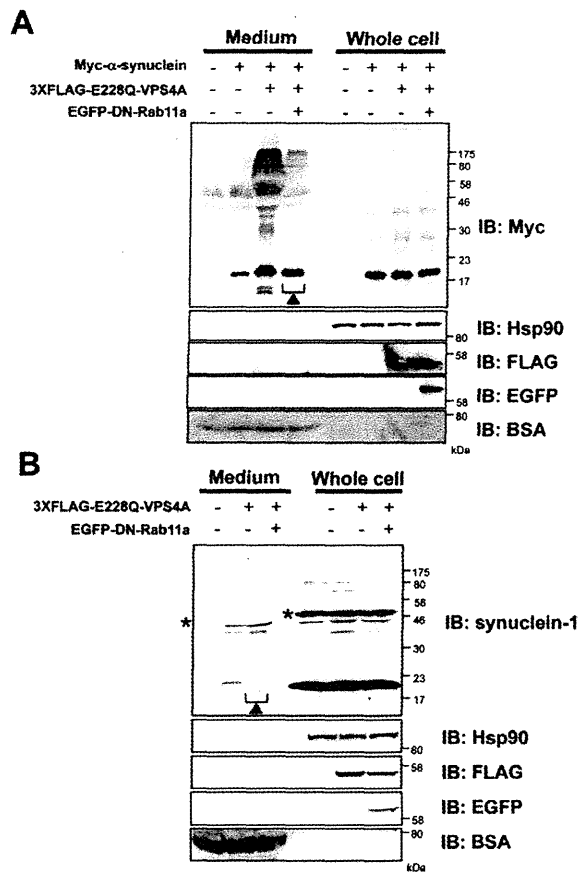
A

B

Figure 7. Increased secretion of α-synuclein by DN-VPS4A is restored by DN-Rab11a. GDP-locked DN-Rab11a strikingly restored the hypersecretion of αSYN triggered by the impaired MVB sorting pathway (*closed triangle*). HEK293T cells co-expressing Myc-αSYN and 3XFLAG-DN-VPS4A (*A*) and SH-SY5Y neuronal cells expressing 3XFLAG-DN-VPS4A (*B*) were further transfected with EGFP-DN-Rab11a. Forty eight hours post transfection, the cells were harvested and solubilized in RIPA buffer. Whole cell lysates as well as total proteins from culture media (50 μg per lane) were then subjected to immunoblot analysis using anti-Myc, anti-synuclein-1, anti-FLAG, and anti-EGFP Abs. Hsp90 and BSA were used as markers for the cytosol and culture medium, respectively. *Asterisk* indicates unspecific band. Representative blots from three independent experiments are presented.
doi:10.1371/journal.pone.0029460.g007

aggregate, level of cellular stress, or the cell-type. Further studies will be needed to gain insight into the cellular mechanisms of disease progression and to identify molecular targets for therapeutic intervention in PD and other neurodegenerative diseases.

Materials and Methods

Plasmid Construction and Preparation

N-terminal Myc-tagged wild-type (wt) αSYN was subcloned into the *Bgl*II and *Not*I sites of pCMV mammalian expression vector (Invitrogen, Carlsbad, CA). For inducible expression, human wt and A53T mutant αSYN cDNAs were introduced into pcDNA4/TO doxycycline (Dox)-inducible expression vector (Invitrogen) using the restriction enzymes *Kpn*I and *Not*I. The plasmid pcDNA6/TR encoding tetracycline repressor protein was purchased as a part of the T-REx tetracycline-regulated mammalian

expression system (Invitrogen). Triple FLAG (3xFLAG)-tagged human wt- and DN E228Q VPS4A were subcloned into the *Eco*RI and *Bam*HI sites of pCMV vector. The pEGFP-C1 plasmids encoding EGFP-tagged human wt-Rab5a, wt-Rab7, wt-Rab11a, CA-Q70L-Rab11a, DN-S25N-Rab11a were kindly provided by Dr. Mitsunori Fukuda (Laboratory of Membrane Trafficking Mechanisms, Department of Developmental Biology and Neurosciences, Tohoku University Biological Institute, Sendai, Japan). Plasmid DNAs were isolated and purified using the GenoPure Plasmid Maxi Kit (Roche, Indianapolis, IN). The fidelity and orientation of the expression constructs were confirmed by restriction enzyme digestion and/or nucleotide sequence analyses.

Cell Culture and Transfection

HEK293T human embryonic kidney cells (kindly gifted by Dr. Taeko Miyagi, Institute of Molecular Biomembrane and Glycobiology, Tohoku Pharmaceutical University, Sendai, Japan) and SH-SY5Y human dopaminergic neuroblastoma cells (CRL-2266; American Type Culture Collection, Manassas, VA) were maintained in Dulbecco's modified Eagle's medium (DMEM; Invitrogen/GIBCO) containing 4.5g/l glucose, 2mM L-glutamine (Invitrogen) supplemented with 10% fetal bovine serum (FBS; Thermo Scientific/HyClone, Rockford, IL) at 37°C under humidified 5% CO_2/air. The SH-SY5Y cell lines in which wt or A53T mutant αSYN can be induced were established using the T-REx expression system which consists of two key expression vectors, pcDNA4/TO and pcDNA6/TR [73,74]. Stably transfected Dox-inducible SH-SY5Y cells were maintained in DMEM containing 4.5g/l glucose, 2mM L-glutamine supplemented with 10% FBS under selective pressure by 5 μg/ml Blasticidin and 300 μg/ml Zeocin (both from InvivoGen, San Diego, CA). HEK293T cells seeded 24 hours prior to transfection were transiently transfected using FuGENE 6 transfection reagent (Roche) at FuGENE 6 (μl)/DNA (μg) ratio of 3:1. SH-SY5Y cells were nucleofected using the Nucleofector I device (LONZA AG, Cologne, Germany) with program A-023. Cells were harvested 48 hours post transfection unless otherwise stated. To evaluate αSYN decay in the presence of lysosomal inhibitor, cells were treated with bafilomycin A1 (0–10 nM dissolved in DMSO; purchased from Sigma) for 24 hours.

Immunofluorescence Confocal Microscopy and Immunohistochemistry

Cells seeded onto UV-sterilized coverslips coated with self-made rat-tail collagen were fixed in 4% (w/v) paraformaldehyde in PBS for 10 min, permeabilized with 0.5% Triton X-100 in PBS for 5min, and blocked with 3% normal goat serum (Wako Pure Chemical Industries, Osaka, Japan) in PBS for 30min. Primary antibodies (rat monoclonal antibody (mAb) anti-DYKDDDDK (FLAG peptide)-tag (1:500; Agilent Technologies, Foster City CA), mouse mAb anti-cMyc (clone 9E10, 1:1000; DSHB, Iowa City, IA), rabbit pAb anti-αSYN (1:1000, CST, Danvers, MA) and mouse mAb anti-LAMP-1 (clone H4A3, 1:1000; DSHB)) were applied for 2 hours followed by anti-mouse IgG Alexa 488 conjugates, anti-rabbit IgG Alexa 568 conjugates, or anti-rat IgG Alexa 647 conjugates (1:2000; Invitrogen/Molecular Probes) for 1 hour. Nuclei were counterstained with TO-PRO3 iodide and pseudo-colored as blue (Invitrogen/Molecular Probes). After immunostaining, coverslips were placed upside down on a drop of PermaFluor antifade mounting medium (Thermo Scientific). Fluorescent images were analyzed with a FV300 confocal laser scanning microscope system equipped with HeNe-Green (543 nm), HeNe-Red (633 nm) and Ar (488 nm) laser units (Olympus Corporation, Tokyo, Japan). In the multiple labeling
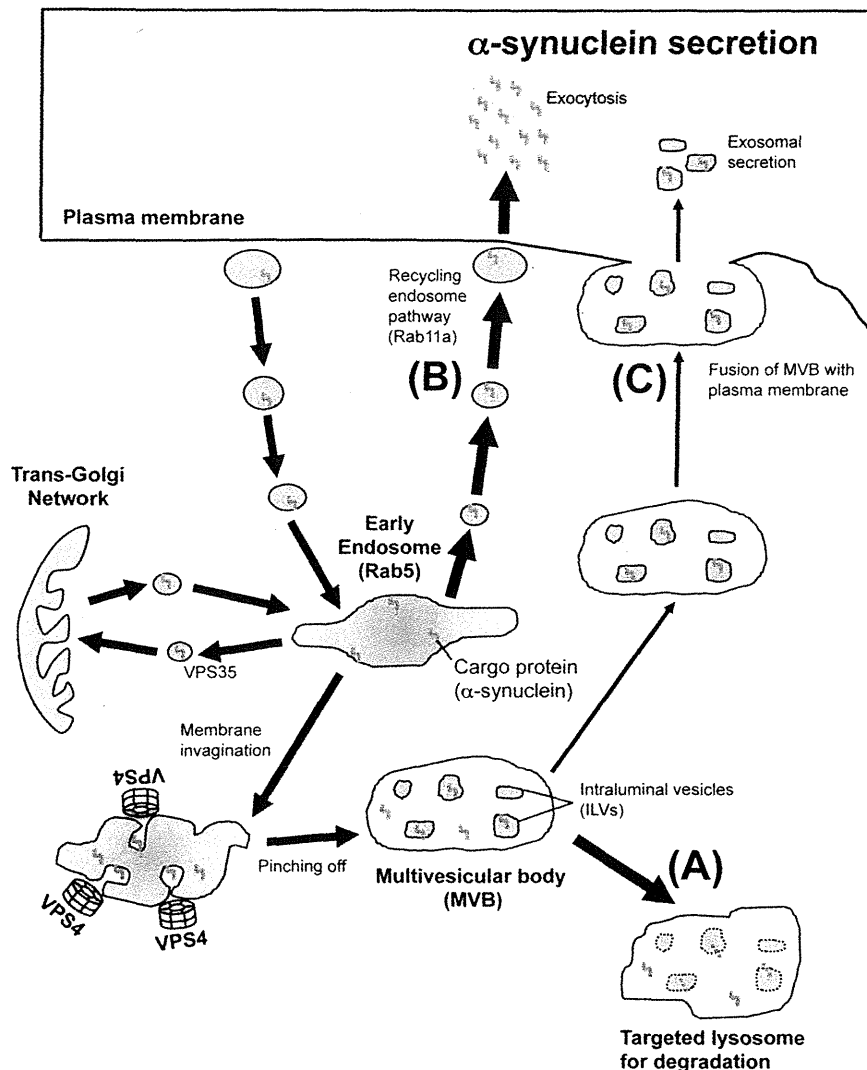
Figure 8. Schematic presentation of endosomal pathways and the functional relevance of MVB sorting machinery and Rab11a-mediated recycling pathway in the secretion as well as lysosomal targeting of α-synuclein. Membrane-associated cargo proteins including αSYN are translocated to early endosomes, which also receive cargoes from the trans-Golgi network. Some cargoes are recycled back to the plasma membrane. Others are sequestered in intraluminal vesicles of MVB. Individual ESCRT proteins and VPS4 contribute to MVB formation through the induction of invagination and final scission of the endosomal membrane. MVB directs either for lysosomal degradation or for secretion as exosomes by exocytic fusion with the plasma membrane. Under the physiolosical condition, αSYN in the early endosome may be transferred to MVB then targeted for lysosomal degradation (A). Alternatively, part of the endosomal αSYN may be cast into the extracellular milieu through the Rab11a-dependent recycling endosome (B) and, to a lesser degree, MVB-exosome pathway (C). If the intracellular αSYN reaches a toxic level or the MVB sorting is dammed up, excessive amounts of endocytic αSYN will flow out mainly through the recycling endosome pathway.
doi:10.1371/journal.pone.0029460.g008

experiments, images were collected using a single excitation for each wavelength separately and then merged using Fluoview image analyzing software (version 4.3, Olympus). For immuno-histochemistry, 4-μm-thick sections of formalin fixed paraffin embedded samples including the substantia nigra and the temporal lobes from patients with PD with a mean age of 77.5 years (n = 4, range 67 to 84 years) and the controls with a mean age of 77.3 y (n = 4, range 67 to 87 years) were subjected to immunohistochemical investigations using the avidin-biotin-per-oxidase complex (ABC) method with a Vectastain ABC kit (Vector Laboratories, Burlingame, CA). Polyclonal Ab against human

VPS4 (SAB4200025, 1:100; Sigma) was used as primary Ab. Diaminobenzidine was used as the chromogen. The sections were counterstained with hematoxylin. No pretreatment of sample before Ab incubation was required.

Subcellular Fractionation by Sequential Centrifugation

For the subcellular fractionation of cultured cells, we adopted an established protocol with slight modifications [75]. All steps of the fractionation scheme were carried out at 0–4°C with ice-cold reagents. Cells (1×10^7) were resuspended with 2 ml ice-cold

fractionation buffer (10 mM Tris/acetic acid pH 7.0, 250 mM sucrose) and homogenized using 20 strokes in a 2-ml Dounce tissue grinder with a tight pestle (GPE, Bedfordshire, England). The cell homogenate was initially cleared by three successive centrifugation steps (500×g for 2 min, 1,000×g for 2 min, 2,000×g for 2 min) to remove debris and undestroyed cells. The supernatant was transferred to a new tube and centrifuged at 4,000×g for 2 min to pellet the plasma membrane and nuclei. The supernatant was ultracentrifuged at 100,000×g (P50S2 swing rotor, Hitachi Koki Co., Ltd., Tokyo, Japan) for 2 min to pellet the mitochondria, endosomes, and lysosomes (fraction EL). Lysosomes were isolated from the fraction EL by 10-min osmotic lysis using five times the pellet volume of distilled water. After another centrifugation step with 100,000×g for 2min, lysosomes remained in the supernatant, while mitochondria and endosomes were in the pellet.

TCA/acetone Protein Extraction from Culture Medium and CSF

Total protein in CM and CSF was extracted by trichloroacetic acid (TCA)/acetone precipitation protocol. Briefly, freshly collected samples were cleared by three successive centrifugation steps (800×g for 5 min, 2,000×g for 10 min, and 10,000×g for 20 min at 4°C) to pellet the debris and intact cells. The supernatant was transferred to a new tube and added with an equal volume of ice-cold 20% TCA/acetone, followed by incubation at −20°C for 3 hours. After adding 3 additional volumes of ice-cold acetone, proteins were allowed to precipitate overnight at −20°C. The protein was pelleted by centrifugation at 5,000×g for 60min, dissolved in 8M urea/5% SDS with sonication, and subjected to Western immunoblot analyses.

Exosome Isolation from Culture Medium and CSF

To isolate exosomes, CM or pooled CSF was collected and subjected to a multi-step differential centrifugation process. In brief, freshly collected samples were subjected to three successive centrifugations at 800×g for 5 min, 2,000×g for 10 min, and 15,000×g for 20 min at 4°C to remove debris and intact cells. After filtration through a 0.22 μm Millipore syringe filter, exosomes were pelleted by ultracentrifugation at 100,000×g (P40ST swing rotor, Hitachi Koki, Co., Ltd.) for 1 hour at 4°C. In some experiments, the exosome-containing pellet was resuspended in ice-cold PBS and further purified by continuous linear sucrose-density gradient centrifugation (2.0–0.25M sucrose, 20 mM HEPES, pH 7.2) according to the method described previously. The exosomal proteins Alix and flotillin-1 were used as markers for the exosome-containing fraction [27].

SDS-Polyacrylamide Gel Electrophoresis and Western Immunoblot Analysis

After preparing the cell lysates using radio-immunoprecipitation assay (RIPA) buffer (1% NP-40, 0.5% deoxycholate, 0.1% sodium dodecyl sulfate (SDS), 1mM EDTA, 10mM sodium pyrophosphate, 50mM sodium fluoride, 1mM sodium orthovanadate, 150mM sodium chloride, 50mM Tris-HCl (pH 8.0) plus 1x Cømplete protease inhibitor cocktail; Roche), the protein concentration was determined using a bicinchoninic acid (BCA) protein assay kit (BioRad, Hercules, CA). Lysates containing 50 μg total protein were boiled in Laemmli loading buffer and then electrophoresed on denaturing 12.5% SDS-polyacrylamide gels using the Mini-PROTEAN 3 cell system (BioRad). Electroblotting onto polyvinylidene fluoride membrane (Immobilon-P; Millipore, Bedford, MA) was performed at 100V for 2 hours. After a blocking step with Tris-Buffer Saline (TBS: 50 mM Tris-HCl, pH 7.5, 150 mM NaCl) with 0.05% Tween 20 (TBST) supplemented with 5% nonfat dry milk, membranes were incubated with anti-cMyc mouse mAb (clone 9E10, 1:1000; DSHB), M2 anti-FLAG/M2 (1:1000; Sigma) mouse mAb, anti-GFP mouse mAb (1:4000; MBL, Nagoya, Japan) anti-synuclein-1 mouse mAb (1:1000; BD Bioscience, San Jose, CA), anti-Alix mouse mAb (clone 3A9, 1:1000; CST), anti-flotillin-1 mouse mAb (1:500; BD Transduction laboratories, Franklin Lakes, NJ), anti-Hsp90 mouse mAb (1:4000; Stressgen, Victoria, BC, Canada), anti-BSA rabbit polyclonal antibody (pAb) (clone B-140, 1:4000; Santa Cruz Biotechnology, Santa Cruz, CA), anti-prion protein mouse mAb (1:1000; Sigma), anti-ubiquitin Ab (clone P4D1, 1:1000; Santa Cruz), anti-LAMP-1 mouse mAb (clone H4A3, 1:1000, DSHB), anti-Rab5 rabbit pAb (1:4000, Santa Cruz), and anti-Rab11 rabbit pAb (1:1000; CST, Danvers, MA). Primary antibodies were followed by horseradish peroxidase-conjugated secondary Ab (1:10000; Jackson ImmunoResearch Laboratories, West Grove, PA). Bands were visualized with Immobilon Western Chemiluminescent HRP Substrate (Millipore) and images were captured by the LAS-3000mini lumino image analyzer (Fujifilm, Tokyo, Japan). Quantification of the band intensity was performed using the Image J version 1.44 software for Mac (developed at the National Institutes of Health, Bethesda, MD) [76]. All experiments were performed at least three times with identical results.

Author Contributions

References

1. Baba M, Nakajo S, Tu PH, Tomita T, Nakaya K, et al. (1998) Aggregation of alpha-synuclein in Lewy bodies of sporadic Parkinson's disease and dementia with Lewy bodies. Am J Pathol 152: 879–884.
2. Hasegawa T, Matsuzaki M, Takeda A, Kikuchi A, Akita H, et al. (2004) Accelerated alpha-synuclein aggregation after differentiation of SH-SY5Y neuroblastoma cells. Brain Res 1013: 51–59.
3. Takeda A, Hasegawa T, Matsuzaki-Kobayashi M, Sugeno N, Kikuchi A, et al. (2006) Mechanisms of neuronal death in synucleinopathy. J Biomed Biotechnol 2006: 19365.
4. Hasegawa T, Matsuzaki-Kobayashi M, Takeda A, Sugeno N, Kikuchi A, et al. (2006) Alpha-synuclein facilitates the toxicity of oxidized catechol metabolites: implications for selective neurodegeneration in Parkinson's disease. FEBS Lett 580: 2147–2152.
5. Sugeno N, Takeda A, Hasegawa T, Kobayashi M, Kikuchi A, et al. (2008) Serine 129 phosphorylation of alpha -synuclein induces unfolded protein response-mediated cell death. J Biol Chem 283: 23179–23188.

6. Iwai A, Masliah E, Yoshimoto M, Ge N, Flanagan L, et al. (1995) The precursor protein of non-A beta component of Alzheimer's disease amyloid is a presynaptic protein of the central nervous system. Neuron 14: 467–475.
7. Clayton DF, George JM (1998) The synucleins: a family of proteins involved in synaptic function, plasticity, neurodegeneration and disease. Trends Neurosci 21: 249–254.
8. Borghi R, Marchese R, Negro A, Marinelli L, Forloni G, et al. (2000) Full length alpha-synuclein is present in cerebrospinal fluid from Parkinson's disease and normal subjects. Neurosci Lett 287: 65–67.
9. El-Agnaf OM, Salem SA, Paleologou KE, Cooper LJ, Fullwood NJ, et al. (2003) Alpha-synuclein implicated in Parkinson's disease is present in extracellular biological fluids, including human plasma. Faseb J 17: 1945–1947.
10. El-Agnaf OM, Salem SA, Paleologou KE, Curran MD, Gibson MJ, et al. (2006) Detection of oligomeric forms of alpha-synuclein protein in human plasma as a potential biomarker for Parkinson's disease. Faseb J 20: 419–425.

11. Tokuda T, Qureshi MM, Ardah MT, Varghese S, Shehab SA, et al. (2010) Detection of elevated levels of alpha-synuclein oligomers in CSF from patients with Parkinson disease. Neurology 75: 1766–1772.

12. Ueda K, Fukushima H, Masliah E, Xia Y, Iwai A, et al. (1993) Molecular cloning of cDNA encoding an unrecognized component of amyloid in Alzheimer disease. Proc Natl Acad Sci U S A 90: 11282–11286.

13. Lee SJ (2008) Origins and effects of extracellular alpha-synuclein: implications in Parkinson's disease. J Mol Neurosci 34: 17–22.

14. Desplats P, Lee HJ, Bae EJ, Patrick C, Rockenstein E, et al. (2009) Inclusion formation and neuronal cell death through neuron-to-neuron transmission of alpha-synuclein. Proc Natl Acad Sci U S A 106: 13010–13015.

15. Lee HJ, Suk JE, Patrick C, Bae EJ, Cho JH, et al. (2010) Direct transfer of alpha-synuclein from neuron to astroglia causes inflammatory responses in synucleinopathies. J Biol Chem 285: 9262–9272.

16. Hansen C, Angot E, Bergstrom AL, Steiner JA, Pieri L, et al. (2011) alpha-Synuclein propagates from mouse brain to grafted dopaminergic neurons and seeds aggregation in cultured human cells. J Clin Invest 121: 715–725.

17. Lee SJ, Desplats P, Sigurdson C, Tsigelny I, Masliah E (2010) Cell-to-cell transmission of non-prion protein aggregates. Nat Rev Neurol 6: 702–706.

18. Kordower JH, Chu Y, Hauser RA, Olanow CW, Freeman TB (2008) Transplanted dopaminergic neurons develop PD pathologic changes: a second case report. Mov Disord 23: 2303–2306.

19. Li JY, Englund E, Holton JL, Soulet D, Hagell P, et al. (2008) Lewy bodies in grafted neurons in subjects with Parkinson's disease suggest host-to-graft disease propagation. Nat Med 14: 501–503.

20. Kordower JH, Chu Y, Hauser RA, Freeman TB, Olanow CW (2008) Lewy body-like pathology in long-term embryonic nigral transplants in Parkinson's disease. Nat Med 14: 504–506.

21. Braak H, Del Tredici K, Rub U, de Vos RA, Jansen Steur EN, et al. (2003) Staging of brain pathology related to sporadic Parkinson's disease. Neurobiol Aging 24: 197–211.

22. Johnstone RM, Adam M, Hammond JR, Orr L, Turbide C (1987) Vesicle formation during reticulocyte maturation. Association of plasma membrane activities with released vesicles (exosomes). J Biol Chem 262: 9412–9420.

23. Fevrier B, Vilette D, Laude H, Raposo G (2005) Exosomes: a bubble ride for prions? Traffic 6: 10–17.

24. Robertson C, Booth SA, Beniac DR, Coulthart MB, Booth TF, et al. (2006) Cellular prion protein is released on exosomes from activated platelets. Blood 107: 3907–3911.

25. Vella LJ, Sharples RA, Lawson VA, Masters CL, Cappai R, et al. (2007) Packaging of prions into exosomes is associated with a novel pathway of PrP processing. J Pathol 211: 582–590.

26. Keller S, Ridinger J, Rupp AK, Janssen JW, Altevogt P (2011) Body fluid derived exosomes as a novel template for clinical diagnostics. J Transl Med 9: 86.

27. Emmanouilidou E, Melachroinou K, Roumeliotis T, Garbis SD, Ntzouni M, et al. (2010) Cell-produced alpha-synuclein is secreted in a calcium-dependent manner by exosomes and impacts neuronal survival. J Neurosci 30: 6838–6851.

28. Alvarez-Erviti L, Seow Y, Schapira AH, Gardiner C, Sargent IL, et al. (2011) Lysosomal dysfunction increases exosome-mediated alpha-synuclein release and transmission. Neurobiol Dis 42: 360–367.

29. Denzer K, Kleijmeer MJ, Heijnen HF, Stoorvogel W, Geuze HJ (2000) Exosome: from internal vesicle of the multivesicular body to intercellular signaling device. J Cell Sci 113(Pt 19): 3365–3374.

30. Johnstone RM (2006) Exosomes biological significance: A concise review. Blood Cells Mol Dis 36: 315–321.

31. Mathivanan S, Ji H, Simpson RJ (2010) Exosomes: extracellular organelles important in intercellular communication. J Proteomics 73: 1907–1920.

32. Slagsvold T, Pattni K, Malerod L, Stenmark H (2006) Endosomal and non-endosomal functions of ESCRT proteins. Trends Cell Biol 16: 317–326.

33. Raiborg C, Stenmark H (2009) The ESCRT machinery in endosomal sorting of ubiquitylated membrane proteins. Nature 458: 445–452.

34. Hurley JH, Hanson PI (2010) Membrane budding and scission by the ESCRT machinery: it's all in the neck. Nat Rev Mol Cell Biol 11: 556–566.

35. Nickerson DP, Russell MR, Odorizzi G (2007) A concentric circle model of multivesicular body cargo sorting. EMBO Rep 8: 644–650.

36. Davies BA, Babst M, Katzmann DJ (2011) Regulation of Vps4 during MVB Sorting and Cytokinesis. Traffic.

37. Beyer A, Scheuring S, Muller S, Mincheva A, Lichter P, et al. (2003) Comparative sequence and expression analyses of four mammalian VPS4 genes. Gene 305: 47–59.

38. Fukuda M (2008) Regulation of secretory vesicle traffic by Rab small GTPases. Cell Mol Life Sci 65: 2801–2813.

39. Stenmark H (2009) Rab GTPases as coordinators of vesicle traffic. Nat Rev Mol Cell Biol 10: 513–525.

40. Matsuzaki M, Hasegawa T, Takeda A, Kikuchi A, Furukawa K, et al. (2004) Histochemical features of stress-induced aggregates in alpha-synuclein overexpressing cells. Brain Res 1004: 83–90.

41. Vella LJ, Greenwood DL, Cappai R, Scheerlinck JP, Hill AF (2008) Enrichment of prion protein in exosomes derived from ovine cerebral spinal fluid. Vet Immunol Immunopathol 124: 385–393.

42. Gough KC, Maddison BC (2010) Prion transmission: prion excretion and occurrence in the environment. Prion 4: 275–282.

43. Porto-Carreiro I, Fevrier B, Paquet S, Vilette D, Raposo G (2005) Prions and exosomes: from PrPc trafficking to PrPsc propagation. Blood Cells Mol Dis 35: 143–148.

44. Scheuring S, Rohricht RA, Schoning-Burkhardt B, Beyer A, Muller S, et al. (2001) Mammalian cells express two VPS4 proteins both of which are involved in intracellular protein trafficking. J Mol Biol 312: 469–480.

45. Morita Y, Sandrin V, Chung HY, Morham SG, Gygi SP, et al. (2007) Human ESCRT and ALIX proteins interact with proteins of the midbody and function in cytokinesis. EMBO J 26: 4215–4227.

46. Cuervo AM, Stefanis L, Fredenburg R, Lansbury PT, Sulzer D (2004) Impaired degradation of mutant alpha-synuclein by chaperone-mediated autophagy. Science 305: 1292–1295.

47. Lee HJ, Suk JE, Bae EJ, Lee JH, Paik SR, et al. (2008) Assembly-dependent endocytosis and clearance of extracellular alpha-synuclein. Int J Biochem Cell Biol 40: 1835–1849.

48. Vogiatzi T, Xilouri M, Vekrellis K, Stefanis L (2008) Wild type a-synuclein is degraded by chaperone mediated autophagy and macroautophagy in neuronal cells. J Biol Chem.

49. Lee HJ, Patel S, Lee SJ (2005) Intravesicular localization and exocytosis of alpha-synuclein and its aggregates. J Neurosci 25: 6016–6024.

50. Liu J, Zhang JP, Shi M, Quinn T, Bradner J, et al. (2009) Rab11a and HSP90 regulate recycling of extracellular alpha-synuclein. J Neurosci 29: 1480–1485.

51. Wikstrom K, Reid HM, Hill M, English KA, O'Keeffe MB, et al. (2008) Recycling of the human prostacyclin receptor is regulated through a direct interaction with Rab11a GTPase. Cell Signal 20: 2332–2346.

52. Peters PJ, Mironov A, Jr., Peretz D, van Donselaar E, Leclerc E, et al. (2003) Trafficking of prion proteins through a caveolae-mediated endosomal pathway. J Cell Biol 162: 703–717.

53. Gousset K, Schiff E, Langevin C, Marijanovic Z, Caputo A, et al. (2009) Prions hijack tunnelling nanotubes for intercellular spread. Nat Cell Biol 11: 328–336.

54. Aguzzi A, Rajendran L (2009) The transcellular spread of cytosolic amyloids, prions, and prionoids. Neuron 64: 783–790.

55. Frost B, Diamond MI (2009) Prion-like mechanisms in neurodegenerative diseases. Nat Rev Neurosci 11: 155–159.

56. Brundin P, Melki R, Kopito R (2010) Prion-like transmission of protein aggregates in neurodegenerative diseases. Nat Rev Mol Cell Biol 11: 301–307.

57. Yamazaki T, Koo EH, Selkoe DJ (1996) Trafficking of cell-surface amyloid beta-protein precursor. II. Endocytosis, recycling and lysosomal targeting detected by immunolocalization. J Cell Sci 109(Pt 5): 999–1008.

58. Lee HJ, Kang SJ, Lee K, Im H (2011) Human alpha-synuclein modulates vesicle trafficking through its interaction with prenylated Rab acceptor protein 1. Biochem Biophys Res Commun.

59. Jo E, McLaurin J, Yip CM, St George-Hyslop P, Fraser PE (2000) alpha-Synuclein membrane interactions and lipid specificity. J Biol Chem 275: 34328–34334.

60. Volles MJ, Lansbury PT, Jr. (2002) Vesicle permeabilization by protofibrillar alpha-synuclein is sensitive to Parkinson's disease-linked mutations and occurs by a pore-like mechanism. Biochemistry 41: 4595–4602.

61. Furukawa K, Matsuzaki-Kobayashi M, Hasegawa T, Kikuchi A, Sugeno N, et al. (2006) Plasma membrane ion permeability induced by mutant alpha-synuclein contributes to the degeneration of neural cells. J Neurochem 97: 1071–1077.

62. Sung JY, Kim J, Paik SR, Park JH, Ahn YS, et al. (2001) Induction of neuronal cell death by Rab5A-dependent endocytosis of alpha-synuclein. J Biol Chem 276: 27441–27448.

63. Lee HJ, Choi C, Lee SJ (2002) Membrane-bound alpha-synuclein has a high aggregation propensity and the ability to seed the aggregation of the cytosolic form. J Biol Chem 277: 671–678.

64. Hayashida K, Oyanagi S, Mizutani Y, Yokochi M (1993) An early cytoplasmic change before Lewy body maturation: an ultrastructural study of the substantia nigra from an autopsy case of juvenile parkinsonism. Acta Neuropathol 85: 445–448.

65. Wakabayashi K, Tanji K, Mori F, Takahashi H (2007) The Lewy body in Parkinson's disease: molecules implicated in the formation and degradation of alpha-synuclein aggregates. Neuropathology 27: 494–506.

66. Shtilerman MD, Ding TT, Lansbury PT, Jr. (2002) Molecular crowding accelerates fibrillization of alpha-synuclein: could an increase in the cytoplasmic protein concentration induce Parkinson's disease? Biochemistry 41: 3855–3860.

67. Hoyer W, Cherny D, Subramaniam V, Jovin TM (2004) Impact of the acidic C-terminal region comprising amino acids 109-140 on alpha-synuclein aggregation in vitro. Biochemistry 43: 16233–16242.

68. Lowe R, Pountney DL, Jensen PH, Gai WP, Voelcker NH (2004) Calcium(II) selectively induces alpha-synuclein annular oligomers via interaction with the C-terminal domain. Protein Sci 13: 3245–3252.

69. Munishkina LA, Cooper EM, Uversky VN, Fink AL (2004) The effect of macromolecular crowding on protein aggregation and amyloid fibril formation. J Mol Recognit 17: 456–464.

70. Duncan LM, Piper S, Dodd RB, Saville MK, Sanderson CM, et al. (2006) Lysine-63-linked ubiquitination is required for endolysosomal degradation of class I molecules. EMBO J 25: 1635–1645.

71. Zimprich A, Benet-Pages A, Struhal W, Graf E, Eck SH, et al. (2011) A Mutation in VPS35, Encoding a Subunit of the Retromer Complex, Causes Late-Onset Parkinson Disease. Am J Hum Genet 89: 168–175.

72. Vilarino-Guell C, Wider C, Ross OA, Dachsel JC, Kachergus JM, et al. (2011) VPS35 Mutations in Parkinson Disease. Am J Hum Genet 89: 162–167.
73. Hasegawa T, Matsuzaki M, Takeda A, Kikuchi A, Furukawa K, et al. (2003) Increased dopamine and its metabolites in SH-SY5Y neuroblastoma cells that express tyrosinase. J Neurochem 87: 470–475.
74. Hasegawa T, Treis A, Patenge N, Fiesel FC, Springer W, et al. (2008) Parkin protects against tyrosinase-mediated dopamine neurotoxicity by suppressing stress-activated protein kinase pathways. J Neurochem 105: 1700–1715.
75. Schroter CJ, Braun M, Englert J, Beck H, Schmid H, et al. (1999) A rapid method to separate endosomes from lysosomal contents using differential centrifugation and hypotonic lysis of lysosomes. J Immunol Methods 227: 161–168.
76. Hasegawa T, Feijoo Carnero C, Wada T, Itoyama Y, Miyagi T (2001) Differential expression of three sialidase genes in rat development. Biochem Biophys Res Commun 280: 726–732.

Plasma L-Cystine/L-Glutamate Imbalance Increases Tumor Necrosis Factor-Alpha from CD14+ Circulating Monocytes in Patients with Advanced Cirrhosis

Eiji Kakazu[1], Yoshiyuki Ueno[1]*, Yasuteru Kondo[1], Jun Inoue[1], Masashi Ninomiya[1], Osamu Kimura[1], Yuta Wakui[1], Koji Fukushima[1], Keiichi Tamai[2], Tooru Shimosegawa[1]

1 Division of Gastroenterology, Tohoku University Graduate School of Medicine, Aobaku, Sendai, Japan, 2 Miyagi Cancer Center, Natori, Japan

Abstract

Background and Aims: The innate immune cells can not normally respond to the pathogen in patients with decompensated cirrhosis. Previous studies reported that antigen-presenting cells take up L-Cystine (L-Cys) and secrete substantial amounts of L-Glutamate (L-Glu) via the transport system Xc- (4F2hc+xCT), and that this exchange influences the immune responses. The aim of this study is to investigate the influence of the plasma L-Cys/L-Glu imbalance observed in patients with advanced cirrhosis on the function of circulating monocytes.

Methods: We used a serum-free culture medium consistent with the average concentrations of plasma amino acids from patients with advanced cirrhosis (ACM), and examined the function of CD14+ monocytes or THP-1 under ACM that contained 0–300 nmol/mL L-Cys with LPS. In patients with advanced cirrhosis, we actually determined the TNF-alpha and xCT mRNA of monocytes, and evaluated the correlation between the plasma L-Cys/L-Glu ratio and TNF-alpha.

Results: The addition of L-Cys significantly increased the production of TNF alpha from monocytes under ACM. Monocytes with LPS and THP-1 expressed xCT and a high level of extracellular L-Cys enhanced L-Cys/L-Glu antiport, and the intracellular GSH/GSSG ratio was decreased. The L-Cys transport was inhibited by excess L-Glu. In patients with advanced cirrhosis (n = 19), the TNF-alpha and xCT mRNA of monocytes were increased according to the Child-Pugh grade. The TNF-alpha mRNA of monocytes was significantly higher in the high L-Cys/L-Glu ratio group than in the low ratio group, and the plasma TNF-alpha was significantly correlated with the L-Cys/L-Glu ratio.

Conclusions: A plasma L-Cys/L-Glu imbalance, which appears in patients with advanced cirrhosis, increased the TNF-alpha from circulating monocytes via increasing the intracellular oxidative stress. These results may reflect the immune abnormality that appears in patients with decompensated cirrhosis.

Introduction

Circulating levels of proinflammatory cytokines such as TNF-alpha, IL-1 beta and IL-6 are increased in patients with cirrhosis [1,2,3]. Endotoxemia has been assumed to be responsible for the increased of such cytokines in patients with cirrhosis [4], because the activation of monocytes, macrophages and dendritc cells (DCs) by lipopolysaccharide (LPS) plays a key role in the pathogenesis of cytokine overproduction. This overproduction of proinflammatory cytokines leads to various complications, such as spontaneous bacterial peritonitis (SBP) and hepatorenal syndrome (HRS) in patients with advanced cirrhosis [5,6].

On the other hand, various types of amino acid imbalance appear in the plasma of patients with decompensated cirrhosis, since the liver plays a major role in metabolism involving glucose, lipids, vitamins, minerals and amino acids. An imbalance of plasma amino acids, with decreased levels of branched-chain amino acids (BCAAs) and increased levels of aromatic amino acids (AAAs), is commonly seen in patients with advanced cirrhosis [7]. Previously, we reported that extracellular branched-chain amino acids (BCAAs) regulate the maturation and function of monocyte derived dendritic cells [8], and that the addition of branched chain amino acids enhances the maturation and function of myeloid dendritic cells ex vivo in patients with advanced cirrhosis [9]. However, it is not clear whether the imbalance of amino acids other than BCAAs influence the immune responses in patients with advanced cirrhosis. A previous study showed that the concentration of plasma L- Cystine (L-Cys) is higher in patients with cirrhosis and shows a wide range of variation [10]. Increased levels of L-Glutamine (L-Gln) and decreasing levels of

L-Glutamate (L-Glu) are seen in patients with advanced cirrhosis, because the L-Glu-L-Gln exchange regulates the high levels of toxic ammonia in such patients [11]. Furthermore, previous studies demonstrated that antigen-presenting cells take up L-Cys via the Na-independent anionic amino acid transport system Xc^- (4F2hc+xCT) and secrete substantial amounts of L-Glu, influencing the immune-responses through this exchange [12,13,14]. This transporter is composed of two protein components, xCT and 4F2hc (CD98), and the transport activity is thought to be mediated by xCT [15,16]. The aim of this study is to investigate the influence of the extracellular L-Cys/L-Glu imbalance observed in patients with advanced cirrhosis on the function of peripheral monocytes using a serum-free culture medium with the average concentration of plasma amino acids from patients with advanced cirrhosis [9], thereby approximating the actual environment of the living body.

Materials and Methods

Ethics Statement

Written informed consent was obtained from each individual and the study protocol was approved by the Ethics Committee of Tohoku University School of Medicine (2009-209, 2009-535).

Monocyte count and isolation

In patients with cirrhosis, the monocyte and lymphocyte counts were measured by a Beckman Coulter LH 750 Analyzer (Fullerton, CA, USA). PBMCs were separated from the peripheral blood of healthy volunteers or patients with cirrhosis by centrifugation on a density gradient. The CD14-positive monocytes were isolated from PBMCs using magnetic microbeads (Miltenyi Biotec, Bergish Gladbach).

The serum free culture media used in this study

A serum free culture medium with the average concentration of plasma amino acids from healthy volunteers (HCM), that from patients with advanced cirrhosis (ACM) and complete culture media (CCM) were described previously [9]. Other components except amino acids were identical among media. Various concentrations of L-Cys were added to L-Cys free ACM , and the final concentration was adjusted to 0–300 nmol/mL (Table S1). We cultured CD14+monocytes, THP-1, Jurkat and Molt-4 under the these media with stimulant and measured the amino acid concentrations of these media. The viability of monocytes and PBMCs was determined using Annexin V^{FITC}, with dead cells identified by propidium iodide (PI) staining (Annexin V^{-FITC} Apoptosis Detection Kit, BioVision, Mountain View, CA), according to the manufacturer's instructions. We confirmed the viability of PBMCs cultured in ACM and ACM plus L-Cys to be equal to that of complete culture medium (CCM) and X-VIVO 10 (Cambrex Bio Science Walkersville, Inc. Walkersville, MD USA).

Patients and Healthy volunteers

The concentrations of the plasma amino acids from fasting patients with chronic hepatitis (n = 17), and patients with cirrhosis (n = 130) were measured by high-performance liquid
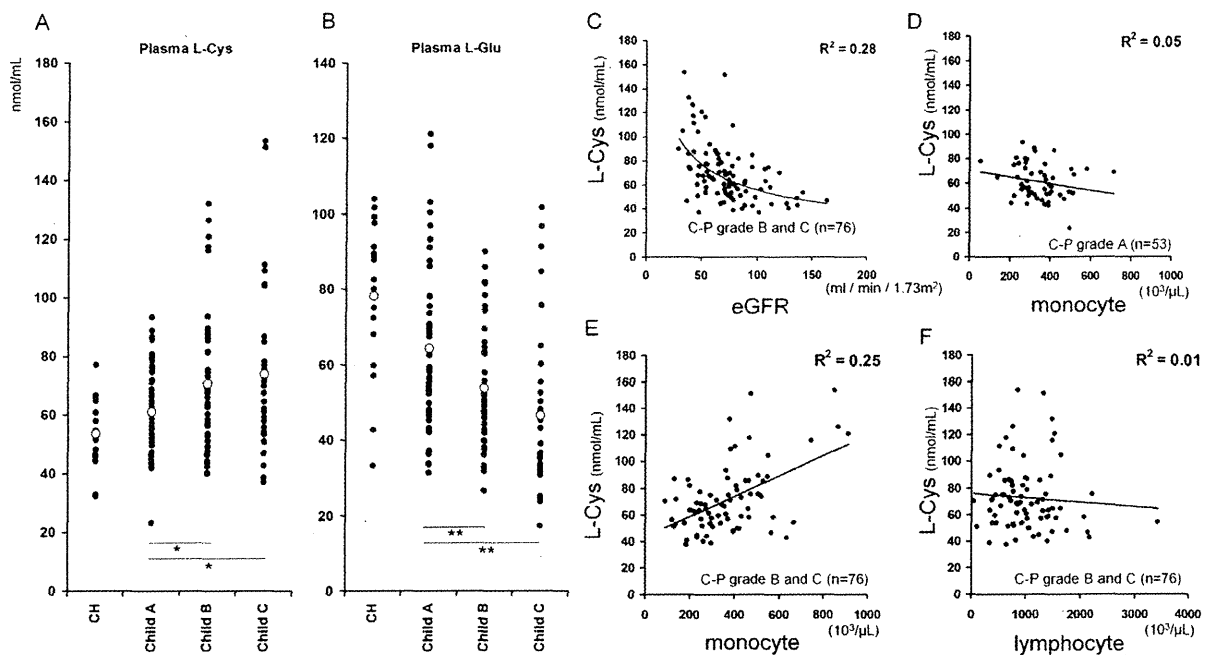

Figure 1. The counts of peripheral monocyte were increased in association with plasma L-Cystine in patients with advanced cirrhosis. A, B, The concentrations of plasma L-Cys in patients with cirrhosis was increased and that of plasma L-Glu was decreased acccording to Child-Pugh grade. The levels of plasma L-Cys and L-Glu in patients with cirrhosis (n = 130) were measured using HPLC and classfied by the Child-Pugh classfication. C, Nonliner regression model was used to model variation in plasma L-Cys and eGFR. D, E,F, Linear regression model was used to model variation in plasma L-Cys and monocyte and lymphocyte counts. Individual correlations between plasma L-Cys levels and monocyte counts in patients with early cirrhosis (D), that in patients with advanced cirrhosis (E), and lymphocyte counts in patients with advanced cirrhosis (F). A,B, **, p<0.01, _*, p<0.05 vs Child-Pugh grade A. Statistical significance was determined by one-way ANOVA and Dunnett's post-hoc procedure. C, D, E, F, R^2 represents coefficient of determination.
doi:10.1371/journal.pone.0023402.g001

A

ACM   ACM+Cys

6

Day 13

20   25.4%   25.5%
            MFI=20056   MFI=20040

B

ACM

ACM+Cys

C

TNF-alpha ng/mL

*

CCM (Cys 200)
HCM (Cys 25)
ACM (Cys 50)
ACM (Cys 100)
ACM (Cys 150)
ACM (Cys 200)
ACM (Cys 300)

D

IL-10 pg/mL

*

CCM
HCM
ACM
ACM+Cys (Cys150)

IFN-γ

CCM
HCM
ACM
ACM+Cys (Cys150)

E

GM-CSF pg/mL

*

CCM
HCM
ACM
ACM+Cys (Cys150)

F

isolated monocytes   2554   725   1662   5589

ACM   45936   14699   4149   11527

ACM+Cys   36309   12310   5923   11215
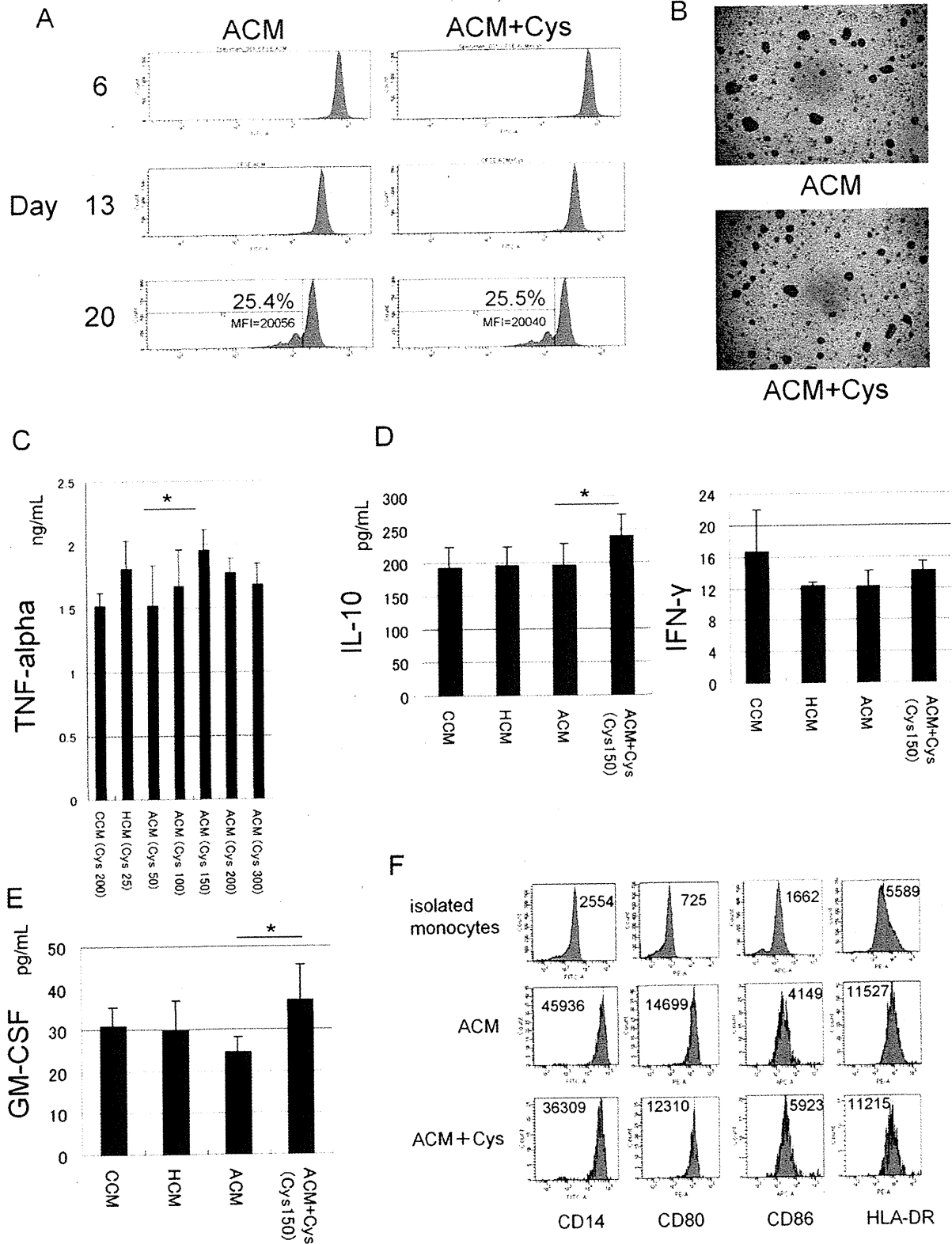
CD14   CD80   CD86   HLA-DR

Figure 2. L-Cystine dose-dependently increased TNF-alpha from CD14+ monocytes with LPS under the amino acid environment of patients with advanced cirrhosis. A, Isolated CD14+ monocytes (purity >90%) were cultured at a density of 2.5×10^5 cells/well in 96-well plates containing in ACM and ACM plus L-Cys (L-Cys : 150 nmol/mL) with 1,000 U/mL M-CSF. One half the amount of culture fluid was exchanged every one day. Cells were maintained for 20 days and the proliferation rate of the cells was measured using CFSE staining. B, Influence of L-Cys on microscopic appearance of monocyte proliferation under serum-free conditions. Day 20, cells in firmly adherent clusters in both ACM and ACM+Cys. C, Monocytes were cultured under CCM, HCM, ACM and ACM plus L-Cys (100–300 nmol/mL). Cells were pre-incubated at a density of 2.5×10^5 cells/well in 96-well flat-bottom plates for 2 hours in each of the media, and 100 ng/mL LPS was added. The supernatants were collected after 24 hours and immediately TNF-alpha was determined by specific cytokine ELISA kits. D,E, Similarly as in Fig. 2C, IL-10, IFN gamma from monocytes and GM-CSF from PBMCs under CCM, HCM, ACM, ACM+Cys (L-Cys 150 nmol/mL) were measured with ELISA. F, Cells were harvested after 24 hours, stained with different mAbs, and analyzed using flow cytometry. Cells were stained with FITC-labeled anti-CD14, -CD80, -CD86, and -HLA-DR. A, B and F results are representative of four experiments from three different donors. C, D and E, Mean ± SEM values from five different donors are shown. C,D,E *, p<0.05 vs ACM (paired Student's t test, two-tailed).
doi:10.1371/journal.pone.0023402.g002

chromatography (HPLC) in the early morning. Briefly, sulfosalicylic acid was added to the plasma to a final concentration of 5%. The samples were then placed on ice for 15 minutes followed by centrifugation to remove precipitated proteins. The extracts were then analyzed for the amino acid content with a JLC-500/V (Japan Electron Optics Laboratories, Tokyo, Japan). Also, the patients with cirrhosis were classified according to the Child-Pugh classification. We defined as Child-Pugh grade B or C the patients with advanced cirrhosis. The estimated glomerular filtration rate (eGFR) was calculated using the new Japanese equation [17].

We selected nineteen patients with cirrhosis for in vitro or ex vivo studies (Table S2). All of these patients were inpatients. The MELD score [18] was calculated by an on-line worksheet available on the internet at www.mayoclinic.org/meld/mayomodel5. html.

Monocyte proliferation assay

Monocytes were cultured at a density of 2.5×10^5 cells/well in 96-well plates containing each media with 1,000 U/mL M-CSF (PEPROTECH EC, London, UK). One half the amount of culture fluid was exchanged every one day. Cells were maintained for 20 days and the proliferation rate of the cells was measured using Carboxyfluorescein Succinimidyl Ester (CFSE) staining; CellTrace CFSE Cell Proliferation Kit (Molecular Probes, Oregon). The staining methods followed the manufacturer's protocol.

Cytokine analysis

PBMCs or monocytes were preincubated at a density of 2.5×10^5 cells/well in 96-well flat-bottom plates (CORNING, NY) for 2 hours in each of the media, and 100 ng/mL LPS (Escherichia coli 026:B6 (SIGMA) were added. The supernatants were collected after 24 hours and immediately TNF-alpha, IFN-gamma, IL-10, GM-CSF were determined by specific cytokine ELISA kits (Bender MedSystems) according to the manufacturer's instructions.

Surface marker analysis

Monocytes were harvested and labeled with FITC-, PE- and APC-labeled monoclonal antibodies (mAbs) (anti-human CD14, CD80, CD86, CD98, HLA-DR, or the relevant isotype controls: BD PharMingen, San Diego, CA), according to the manufacturer's instructions. On xCT expression, indirect staining was performed; primary antibody (xCT (H-121) scc-98552: Santa Cruz) secondary antibody (goat anti-rabbit IgG-FITC sc-2012: Santa Cruz) Using a FACS Canto II (BD Immunocytometry Systems, San Diego, CA) flow cytometer, surface marker expressions were analyzed using the BD FACSDiva (BD Immunocytometry Systems) program.

Intra-extracellular amino acid quantification

The THP-1, Jurkat and Molt4 cells were pre-incubated for 2 hr in ACM, then 1.0×10^7 cells were re-suspended with LPS

(100 ng/mL) or IL-2 (1000 IU/mL) in 1 mL of ACM, L-Cys-free ACM or ACM with L-Cys. After 2 hr incubation, the supernatants were measured by HPLC for the extracellular amino acid quantification. The concentration of the intracellular amino acids was determined as described in ref [19]. Briefly, cells were washed two times by PBS and resuspended in 500 µL PBS sonicated with four 10-s pulses. Cell debris was removed by centrifugation, and sulfosalicylic acid was added to the supernatant to a final concentration of 2%. The samples were then placed on ice for 30 min followed by centrifugation to remove precipitated proteins. The extracts were then analyzed for amino acid content with an L-8500 amino acid analyzer (Hitachi Ltd., Tokyo).

Measurement of reduced glutathione (GSH) and oxidized glutathione (GSSG)

CD14+ monocytes were pre incubated at a density of 2.0×10^5 cells/well in 96-well plates containing HCM for 2 h and then cultured in HCM, ACM or ACM plus L-Cys for an additional 2 h. The culture medium was carefully removed from the wells. 100 µl of prepared GSH-Glo™ Reagent were added to each well of a 96-well plate, mixed briefly on a plate shaker, and incubated at room temperature for 30 minutes. 100 µl of reconstituted Luciferin Detection Reagent were added to each well of a 96-well plate, mixed briefly on a plate shaker, and incubated for 15 minutes. luminescence was read by a Lumino Skan Ascent (Thermo BioAnalysis, Helsinki, Finland).

Real-time PCR

THP-1, Jurkat, Molt-4 and CD14+ monocytes were collected. After the extraction of total RNA and the RT procedure, real-time PCR using a TaqMan Chemistry System () was carried out. The ready-made sets of primers and probes for the amplification of xCT (Assay ID : Hs00921937_m1), TNF-alpha (Assay ID : Hs99999043_m1) and glyceraldehyde-3-phosphate-dehydrogenase (GAPDH, Assay ID : Hs02758991_g1) were purchased from Perkin-Elmer/Applied Biosystems. The relative amount of target mRNA was obtained by using a comparative threshold cycle (CT) method. The expression level of mRNAs of the Molt-4 was represented as 1.0 and the relative amounts of target mRNA in THP-1 and Jurkat were calculated according to the manufacturer's protocol. For CD14+ monocytes, The expression level of monocyte mRNA from a healthy volunteer was represented as 1.0 and the relative amounts of target mRNA in monocytes from patients were calculated.

Statistical Analysis

The data were analyzed with ANOVA, and multiple comparisons were performed with Dunnett's post-hoc procedure for the plasma aminogram. When 2 groups were analyzed, the differences between media were analyzed by the Wilcoxon t test, and the

5